

One-parameter dynamical dark energy: Hints for oscillations

Daniel A. Kessler,^{1,*} Luis A. Escamilla,^{1,†} Supriya Pan,^{2,3,‡} and Eleonora Di Valentino^{1,§}

¹*School of Mathematical and Physical Sciences, University of Sheffield,
Hounsfield Road, Sheffield S3 7RH, United Kingdom*

²*Department of Mathematics, Presidency University, 86/1 College Street, Kolkata 700073, India*

³*Institute of Systems Science, Durban University of Technology,
PO Box 1334, Durban 4000, Republic of South Africa*

There is mounting evidence from multiple cosmological probes that dark energy may be dynamical, with an equation of state that evolves over cosmic time. While this evidence is typically quantified using the Chevallier–Polarski–Linder (CPL) parametrization, based on a linear expansion of $w(a)$ in the scale factor, non-parametric reconstructions frequently suggest non-linear features, particularly at late times. In this work, we investigate four minimal one-parameter models of dark energy with non-linear dependence on the scale factor. These models are constrained using Cosmic Microwave Background (CMB) data from *Planck*, lensing reconstruction from ACT-DR6, Baryon Acoustic Oscillation (BAO) measurements from DESI-DR2, and three Type-Ia supernovae (SNe) samples (PantheonPlus, DESY5, and Union3), considered independently. Although our conclusions depend on the choice of SNe sample, we consistently find a preference, as measured by the chi-squared statistic and the Bayesian evidence, for these dynamical dark energy models over the standard Λ CDM model. Notably, with the PantheonPlus dataset, one model shows strong Bayesian evidence ($\Delta \ln B \simeq 4.5$) against CPL, favoring an equation of state that peaks near $a \simeq 0.7$ and oscillates near the present day. These results highlight the impact of SNe selection and contribute to the growing collection of evidence for late-time deviations from Λ CDM.

I. INTRODUCTION

The discovery of the late-time accelerated expansion of the universe [1, 2] significantly unbalanced our understanding of the physical laws and fundamental fields behind cosmic evolution. In a statistically homogeneous and isotropic universe, these observations are most easily explained by a hypothetical fluid with negative pressure (referred to as *dark energy*), traditionally characterized by a positive cosmological constant Λ with an equation of state $w_\Lambda = -1$. Theoretical objections to this constant, such as its apparent inconsistency with modern particle physics [3] and seemingly fine-tuned initial conditions [4], have long inspired speculation on a more fundamentally sound explanation for the observed late-time expansion [5, 6]. Despite this, no alternative to Λ has garnered widespread consensus, and the current cosmological standard model (Λ CDM) assumes the cosmological constant hypothesis is exactly correct.

Increasingly in the past decade, precision cosmological data have revealed observational tensions within the Λ CDM paradigm. These notably include the $> 5\sigma$ disagreement between Hubble constant (H_0) measurements from the *Planck* cosmic microwave background (CMB) satellite [7] and local distance-ladder estimates from the SH0ES collaboration [8–10], as well as the tension between the galactic-scale matter clustering inferred by *Planck* [7] (quantified by the S_8 parameter [11, 12]) and

estimates derived directly from galaxy surveys and weak gravitational lensing observations [13–28], which was recently alleviated by the new KiDS-Legacy release [29]. Nonetheless, such inconsistencies suggest that the assumptions of the standard cosmological model could be refined or replaced with ones that have greater observational support.¹

When investigating alternatives to Λ , two phenomenological approaches are commonly employed. The first is *parametric* and involves assuming a specific functional form for, e.g., the dark energy equation of state, $w(a)$, as a function of cosmic time, here measured by the scale factor a . This function typically includes one or more free parameters, which are constrained using observational data [35–111]. Alternatively, *non-parametric* methods use numerical and statistical tools to *reconstruct*, e.g., $w(a)$ in different scale factor or redshift ranges [112–121]. Whereas non-parametric methods are more flexible, parametric models can often achieve tighter constraints on their (fewer) degrees of freedom. Within the parametric approach, there are two standard choices for the form of the dark energy equation of state: the constant w CDM model and the dynamical w_0w_a or Chevallier–Polarski–Linder (CPL) parametrization [122, 123], which arise from Taylor expanding a general $w(a)$ to zeroth and linear order, respectively.²

Assuming the CPL parametrization, the Dark Energy Spectroscopic Instrument (DESI) collaboration recently reported a 2.8–4.2 σ preference for dynamical dark en-

* ph4dke@sheffield.ac.uk

† l.a.escamilla@sheffield.ac.uk

‡ supriya.maths@presiuniv.ac.in

§ e.divalentino@sheffield.ac.uk

¹ See [30–34] for reviews of attempts in this direction.

² The CPL parametrization was also proposed to capture the behavior of more fundamental (scalar field) models [122].

ergy when combining their own baryon acoustic oscillation (BAO) measurements [124–126] with CMB data from *Planck* [7] and different Type-Ia supernovae (SNe) catalogs [127–132]. The first DESI data release [133–135] prompted much discussion on the robustness and implications of these BAO and SNe data [136–165]. Importantly, the evidence for dynamical dark energy was confirmed using dataset combinations that do not include DESI BAO measurements [166]³ and parameterizations other than CPL [167–169].

There are several reasons to consider parameterizations beyond CPL when evaluating the evidence for a dynamical $w(a)$. While this parametrization is limited to a purely linear evolution and diverges in the infinite future ($a \rightarrow \infty$), alternatives such as the Barboza–Alcaniz proposal [57] address both of these potential shortcomings. Notably, this alternative was favored over CPL by the datasets used in the original DESI analysis [168]. Furthermore, non-parametric reconstructions of the dark energy equation of state consistently find oscillating features during late times ($a \gtrsim 2/3$) [115–117, 119–121, 170], this feature being inconsistent with linear evolution and in qualitative agreement with the general parametrization in [97]. In view of these preferences, we consider alternative parameterizations for $w(a)$ that evolve non-monotonically with a and are well-defined throughout all cosmic history.

An important consideration in phenomenological studies of dark energy is the number of free parameters introduced in the equation of state. This decision is less ambiguous in more fundamental approaches, where parameters come from the underlying microphysics [171], and in the w CDM and CPL parameterizations, which follow from a general series expansion of $w(a)$. For alternative phenomenological models, the optimal number of parameters depends on the goals of the study. When attempting to constrain multiple independent features of $w(a)$ (e.g., its present-day value, phantom crossing, and oscillations), having two or more parameters is justified and likely required for accurate conclusions. However, models with more phenomenological parameters often have a more degenerate parameter space and worse Bayesian evidence, as the necessarily agnostic priors on the new parameters significantly increase the prior volume. Because our concern is identifying alternatives to Λ that provide a better fit to modern cosmological data according to both the chi-squared statistic and Bayesian evidence, we consider parameterizations of the dark energy equation of state with only a single free parameter. Our results demonstrate that some such models are preferred over traditional parameterizations by current CMB, BAO, and Type-Ia SNe data.

This paper is organized as follows. In Section II, we

review the cosmological effects of dark energy and introduce the models considered in this work. Section III presents the observational data used in our analyses, and Section IV discusses the resulting observational constraints on the dark energy parameterizations. Finally, Section V summarizes our main findings and concludes.

II. DARK ENERGY

Assuming a spatially flat Friedmann-Lemaître-Robertson-Walker (FLRW) universe, general relativity predicts the Friedmann equation

$$H(a) = H_0 \left[\Omega_m a^{-3} + \Omega_\gamma a^{-4} + \Omega_\nu \frac{\rho_\nu(a)}{\rho_{\nu,0}} + \Omega_{\text{DE}} \frac{\rho_{\text{DE}}(a)}{\rho_{\text{DE},0}} \right]^{1/2}, \quad (1)$$

for the Hubble parameter $H(a) \equiv (da/dt)/a$, where t is cosmic time, a is the scale factor, $\Omega \equiv \rho_{\cdot,0}/(3H_0^2/8\pi G)$, $\Omega_m \equiv \Omega_b + \Omega_c$, and we have chosen the present-day scale factor $a_0 \equiv 1$. In these equations, a zero subscript implies evaluation at present, while the subscripts b , c , γ , ν , and DE refer to baryons, cold dark matter, photons, neutrinos, and dark energy, respectively. Assuming that dark energy does not interact with the other components and is minimally coupled to gravity, its energy density obeys the evolution equation

$$\frac{\rho_{\text{DE}}(a)}{\rho_{\text{DE},0}} = a^{-3} \exp \left[3 \int_a^1 da' \frac{w(a')}{a'} \right], \quad (2)$$

where $w(a)$ is the (barotropic) dark energy equation of state. Given a specific model for $w(a)$, Eqs. (1) and (2) determine the background geometry of the universe.

To model dark energy perturbations, we use the default parameterized post-Friedmann (PPF) method implemented in the Boltzmann code CAMB [172], which allows $w(a)$ to cross the phantom divide ($w = -1$) without introducing divergences in the perturbation equations [173, 174]. In the PPF framework, a free function Γ parametrizes deviations from the evolution of metric perturbations in a universe without dark energy. By requiring that these deviations are consistent with a spatially flat FLRW background on super-horizon scales, satisfy local energy–momentum conservation, and are fully suppressed on small scales, Refs. [173, 174] derive the defining and evolution equations for Γ :

$$\Gamma = -4\pi G \left(\frac{a}{k} \right)^2 \rho_{\text{DE}} \delta_{\text{DE}}^{(\text{rest})}, \quad (3)$$

$$(1 + c_\Gamma^2 k_H^2) \left[\frac{d\Gamma}{d(\ln a)} + (1 + c_\Gamma^2 k_H^2) \Gamma \right] = S, \quad (4)$$

where $\delta_{\text{DE}}^{(\text{rest})} \equiv (\delta\rho_{\text{DE}}/\rho_{\text{DE}})^{(\text{rest})}$ is evaluated in the dark energy rest frame, and c_Γ determines the scale at which

³ The strength of evidence is driven largely by the SNe catalog. In particular, DES 5-year SNe data [130] already show a preference for dynamical dark energy.

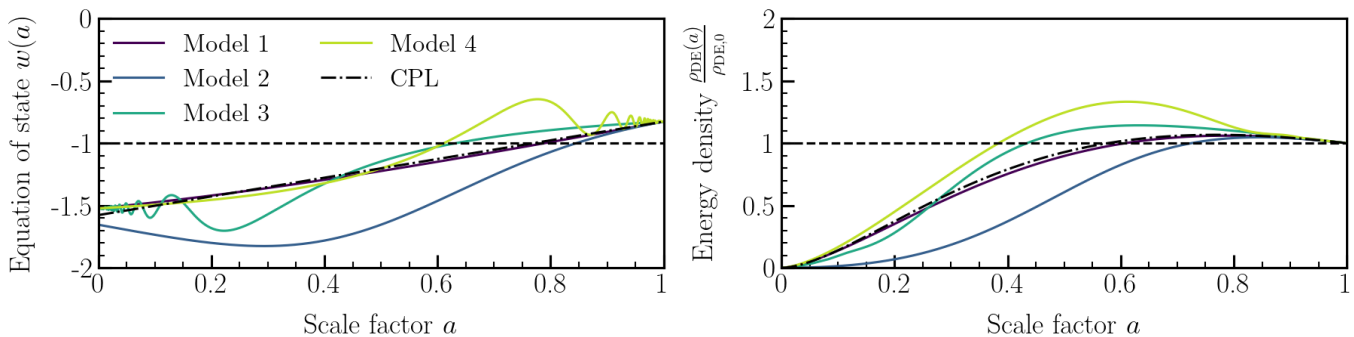


FIG. 1. The $w(a)$ and $\rho_{DE}(a)/\rho_{DE,0}$ for each dark energy model considered in this work [Eqs. (5)–(8)] are compared with the mean quantities obtained by DESI [124] using the CPL parametrization and the *Planck* 2018, ACT-DR6 Lensing, DESI-DR2 BAO, and PantheonPlus dataset combination (dash-dot lines). Each dark energy model is shown with the same present-day value of $w(a)$, and the horizontal dashed lines represent the Λ CDM predictions.

dark energy becomes smooth relative to matter.⁴ The quantity $k_H = k/(aH)$ is the physical wavenumber relative to the Hubble parameter, and the source term S in Eq. (4) includes contributions from $\rho_{DE}(a)$ and $w(a)$, alongside velocity perturbations in the matter sector [174].

A. Models

We consider four one-parameter models of the dark energy equation of state, motivated by their simplicity and the preferences found in previous studies:

$$\text{Model 1: } w(a) = w_0 [1 + \sin(1 - a)] \quad (5)$$

$$\text{Model 2: } w(a) = w_0 \left[1 + \frac{1 - a}{a^2 + (1 - a)^2} \right] \quad (6)$$

$$\text{Model 3: } w(a) = w_0 \left[1 - a \sin\left(\frac{1}{a}\right) + \sin 1 \right] \quad (7)$$

$$\text{Model 4: } w(a) = w_0 \left[1 + (1 - a) \sin\left(\frac{1}{1 - a}\right) \right]. \quad (8)$$

The equation of state and the corresponding energy density, $\rho_{DE}(a)$, for each model are depicted in Fig. 1. These models have increasing shapes⁵ that can be shifted vertically and modulated in amplitude by varying their single parameter, w_0 , which also represents the present-day value of $w(a)$. The variation of each equation of state with w_0 is shown in the top panel of Fig. 2. Although

every model is well-defined and includes some oscillations over the entire history of the universe, corresponding to $a \in [0, \infty)$, only Models 2 through 4 have oscillations within the time domain $a \in [0, 1]$ that is relevant to our analysis.

The first parametrization (Model 1) was explored in [79] and arises from a simple elementary function (the sine function) that does not require an additional parameter to control the slope: its average slope naturally aligns with the CPL preference found by DESI [124]. This model has the lowest frequency of oscillations and is the only one to remain monotonic over $a \in [0, 1]$. Model 2 is obtained by equating the two parameters of the Barboza–Alcaniz proposal [57]. This model has a single “oscillation,” decreasing until $a \sim 0.3$ before increasing toward the present day.

The last two equations of state (Models 3 and 4) are inspired by the oscillating parametrization introduced by Ma and Zhang [60]. In both models, a linear envelope is supplemented by oscillations that rapidly increase in frequency after the beginning of the universe (Model 3) or before the present day (Model 4). Whereas the former model is obtained by equating the parameters of the Ma–Zhang equation of state, the latter has (to our knowledge) not been analyzed previously in the literature. Model 4 is further notable for its ability to capture both the phantom crossing preferred by parametric studies and the late-time extrema and oscillations found in non-parametric reconstructions [115–117, 119–121, 170].

The bottom panel of Fig. 2 illustrates the impact of these dark energy models on the CMB TT and EE power spectra. Explicitly, these spectra were obtained assuming Model 1. However, the other models yield similar results, with the most noticeable differences appearing in the low- ℓ plateau (due to the late-time Integrated Sachs–Wolfe effect) and the high- ℓ damping tail (due to the geometrical degeneracy between w_0 and H_0). These differences are limited to around 5% and 10%, respectively, when the equation of state parameter is restricted to the range $w_0 \in [-1, -0.65]$ that is preferred by our

⁴ Calibrating the PPF formalism on scalar field models of dark energy gives $c_T = 0.4 c_{DE}$ [174], where c_{DE} is the dark energy sound speed. This is the default value chosen by CAMB.

⁵ Decreasing equations of state are not considered, as they are disfavored by current cosmological data. Using the CPL parametrization, the DESI collaboration found that $w_a < 0$ at greater than 2.5σ significance. We have further confirmed that the decreasing versions of Models 1 and 4 provide significantly worse fits to the datasets we consider.

analysis (Section IV). Since Model 3 affects the CMB in much the same way as Model 1, its early-time oscillations are not expected to significantly affect its fit to the datasets we consider. Conversely, the late-time oscillations of Model 4 should be resolvable through the BAO and SNe distance measurements.

III. OBSERVATIONAL DATA AND METHODOLOGY

To perform parameter inference, we use the publicly available Markov Chain Monte Carlo (MCMC) sampler `Cobaya` [175] in conjunction with the Boltzmann solver `CAMB` [172], modified to incorporate our dark energy parameterizations. We assess the convergence of our MCMC chains using the Gelman–Rubin diagnostic parameter, $R - 1$ [176], and consider the chains to be converged when the criterion $R - 1 < 0.02$ is met. The MCMC results are analyzed and plotted using `getdist` [177].

Our models extend the standard Λ CDM framework by introducing an additional parameter for the dark energy equation of state, bringing the total number of free parameters to seven. These are: the physical baryon density $\Omega_b h^2$, the physical dark matter density $\Omega_c h^2$, the optical depth to reionization τ , the angular size of the sound horizon at recombination θ_s , the amplitude of primordial scalar perturbations $\log(10^{10} A_s)$, the scalar spectral index n_s , and the equation of state parameter w_0 . For all parameters, we assume the flat (uninformative) priors given in Table I.

Parameter	Prior
$\Omega_b h^2$	[0.005, 0.1]
$\Omega_c h^2$	[0.005, 0.99]
τ	[0.01, 0.8]
$100 \theta_s$	[0.5, 10]
$\log(10^{10} A_s)$	[1.61, 3.91]
n_s	[0.8, 1.2]
w_0	[-2, 0]

TABLE I. The flat prior distributions imposed on the cosmological parameters in our analyses. We assume the prior $w_a \in [-3, 2]$ for the additional parameter of the CPL model.

To constrain these parameters, we use the following datasets:

- Cosmic Microwave Background (CMB) temperature anisotropy and polarization power spectra, their cross-spectra, and the reconstructed lensing from the *Planck* 2018 legacy data release [7, 178–180]. This dataset is referred to as **Planck 2018**.

- The sixth data release of the CMB lensing power spectrum from the Atacama Cosmology Telescope [181, 182], which incorporates measurements from *Planck*.⁶ This dataset is referred to as **ACT-DR6 Lensing**.
- Baryon Acoustic Oscillation (BAO) measurements from the first two years of observations by the Dark Energy Spectroscopic Instrument (DESI) [124–126]. This dataset is referred to as **DESI-DR2 BAO**.

These three datasets (*Planck* 2018, ACT-DR6 Lensing, and DESI-DR2 BAO) form our “baseline” for parameter inference and are included in all analyses. In contrast, the next three datasets consist of different Type-Ia SNe samples, which are not used simultaneously. These are:

- A total of 1701 light curves from 1550 distinct SNe spanning the redshift range $0.01 < z < 2.26$, obtained from the PantheonPlus sample [127, 128]. This dataset is referred to as **PantheonPlus**.
- The full 5-year dataset of the Dark Energy Survey (DES) Supernova Program, which includes distance modulus measurements for 1635 SNe in the redshift range $0.1 < z < 1.13$ [129–131]. This dataset is referred to as **DES5**.
- The Union3 compilation, consisting of 2087 SNe [132]. This dataset is referred to as **Union3**.

A. Model Preference Statistics

To quantify the preference (or lack thereof) of these datasets for the dark energy models in Eqs. (5)–(8) compared to Λ CDM and the CPL parametrization, we use two statistical measures: the change in the minimum (best-fitting) chi-squared, $\Delta\chi_{\min}^2$, and the logarithmic Bayesian evidence ratio, $\Delta \ln B$:

$$\Delta\chi_{\min}^2 \equiv \min \chi_{\text{Model } i}^2 - \min \chi_{\Lambda\text{CDM or CPL}}^2, \quad (9)$$

$$\Delta \ln B \equiv \ln \left[\frac{B_{\text{Model } i}}{B_{\Lambda\text{CDM or CPL}}} \right], \quad (10)$$

where both χ_{\min}^2 and the Bayesian evidence B are obtained directly from our MCMC chains, with the latter computed using `MCEvidence` [183] and the `Cobaya` wrapper in the `wgcosmo` repository [184]. A model provides a better fit to the data according to the chi-squared statistic if $\Delta\chi_{\min}^2 < 0$,⁷ while a Bayesian preference is theoretically indicated by $\Delta \ln B > 0$.

⁶ We use the `actplanck_baseline` likelihood variant from https://github.com/ACTCollaboration/act_dr6_lenslike.

⁷ We cannot strictly apply Wilks’ theorem to perform a likelihood ratio test—deriving a p -value and corresponding “ σ ” significance from $\Delta\chi_{\min}^2$ —because Λ CDM and CPL are not nested within our one-parameter models.

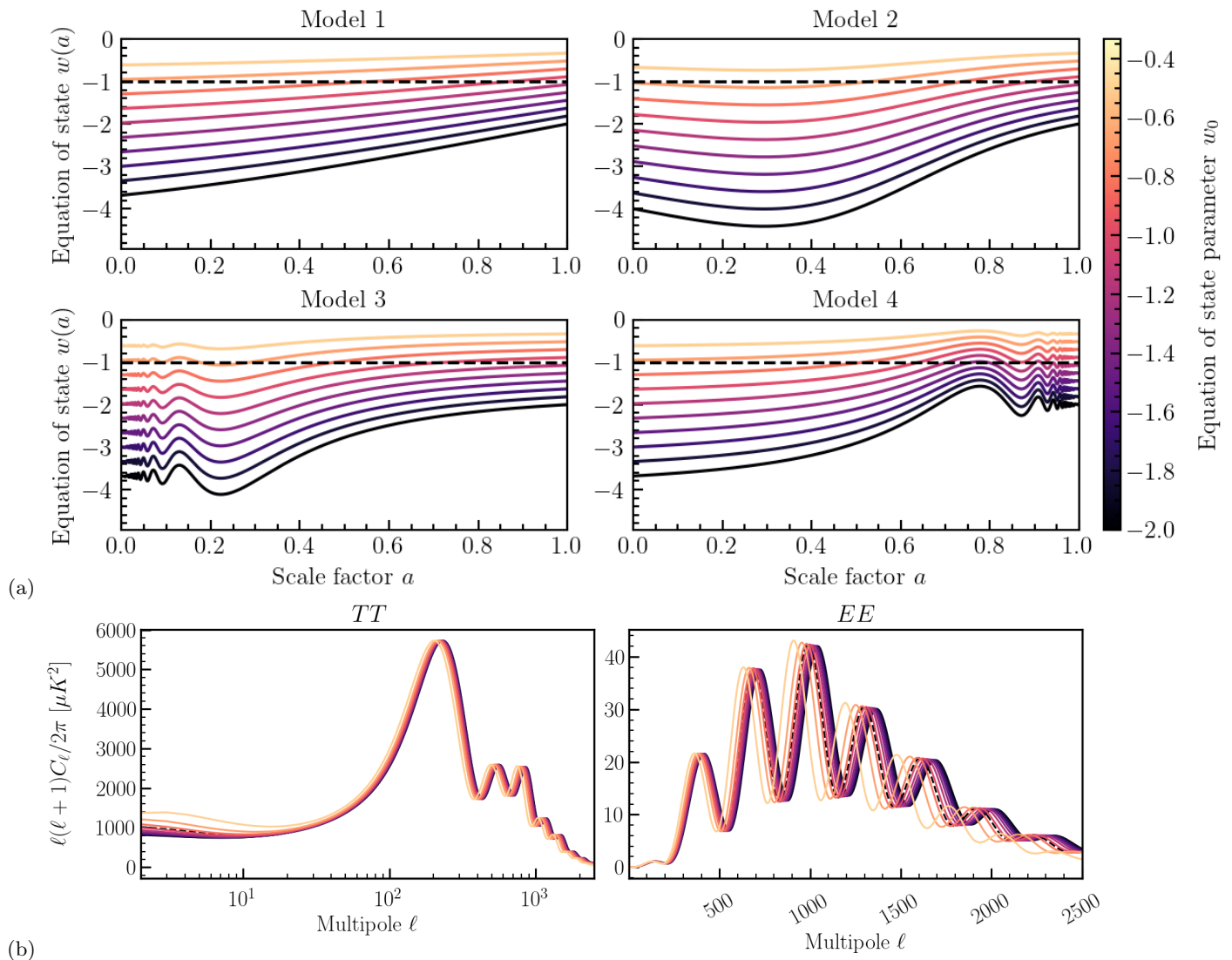


FIG. 2. (a) The equation of state of each dark energy model when w_0 is varied in the range $[-2, -1/3]$. (b) The corresponding effect of Model 1 on the CMB TT and EE power spectra. Here, w_0 is varied while fixing the six Λ CDM parameters to their *Planck* 2018 values, and the dashed lines show the best-fitting Λ CDM spectra. The results for the other three models are similar, with small differences ($\lesssim 5\%$) in the low- ℓ TT spectrum, due to the ISW effect, and slightly larger differences ($\lesssim 10\%$) in the high- ℓ TT spectrum, due to the geometrical degeneracy between w_0 and H_0 , when w_0 is restricted to the range $w_0 \in [-1, -0.65]$ that is preferred by our analysis (Section IV).

Unlike the minimum chi-squared, the Bayes ratio accounts for the number of free parameters and prior ranges of the models, penalizing those with larger prior volumes and greater complexity. To interpret the Bayesian evidence, we refer to the revised Jeffreys' scale [185], where $|\Delta \ln B| \lesssim 1$ is considered inconclusive, $1 \lesssim |\Delta \ln B| \lesssim 3$ indicates moderate evidence, and $3 \lesssim |\Delta \ln B| \lesssim 5$ corresponds to strong evidence.

IV. RESULTS

In this section, we present observational constraints on the four dark energy models in Eqs. (5)–(8) and evaluate

their model preference statistics compared to Λ CDM and the CPL parametrization, using the methodology outlined in the previous section. The posterior distributions of the dark energy equation of state parameter w_0 , the Hubble constant H_0 , and the matter fluctuation parameter S_8 are shown in Figs. 3–6, alongside the best-fitting dark energy equation of state $w(a)$, for each dataset combination. Observational constraints on each model's energy density $\rho_{\text{DE}}(a)$ are compared in Fig. 7. Complete information on the models' seven free parameters and relevant derived parameters is given in Tables II–V. Finally, the model preference statistics are summarized in Table VI and Fig. 8, which provides a useful visual depiction.

Parameter	PantheonPlus	DESY5	Union3
$\Omega_c h^2$	0.11932 ± 0.00075	0.11898 ± 0.00075	0.11884 ± 0.00077
$\Omega_b h^2$	0.02243 ± 0.00013	0.02245 ± 0.00013	0.02247 ± 0.00013
$100\theta_{MC}$	1.04100 ± 0.00028	1.04105 ± 0.00029	1.04107 ± 0.00029
τ_{reio}	0.0553 ± 0.0071	0.0565 ± 0.0071	$0.0570^{+0.0068}_{-0.0077}$
n_s	0.9672 ± 0.0034	0.9680 ± 0.0035	0.9683 ± 0.0035
$\log(10^{10} A_s)$	3.045 ± 0.013	3.047 ± 0.013	3.049 ± 0.013
w_0	-0.795 ± 0.021	-0.773 ± 0.019	-0.762 ± 0.024
Ω_m	0.3126 ± 0.0053	0.3175 ± 0.0051	0.3199 ± 0.0062
σ_8	0.8125 ± 0.0086	0.8053 ± 0.0081	0.8021 ± 0.0095
S_8	0.8293 ± 0.0076	0.8284 ± 0.0077	0.8282 ± 0.0077
H_0	67.50 ± 0.59	66.90 ± 0.54	66.62 ± 0.68
τ_{drag}	147.22 ± 0.20	147.28 ± 0.20	147.30 ± 0.21
$\Delta\chi^2_{min} (\Delta \ln B) \Lambda\text{CDM}$	-8.2 (-0.0)	-19.3 (5.6)	-12.8 (3.3)
$\Delta\chi^2_{min} (\Delta \ln B) \text{CPL}$	1.0 (1.8)	-0.4 (2.1)	0.8 (1.2)

TABLE II. **Model 1.** Constraints (68% CL) on the seven free parameters listed in Table I, alongside relevant derived parameters, using the combination of our baseline dataset with each of the three Type-Ia SNe samples (PantheonPlus, DESY5, and Union3) separately. The minimum chi-squared difference, $\Delta\chi^2_{min}$ [Eq. (9)], and the logarithmic Bayesian evidence ratio, $\Delta \ln B$ [Eq. (10)], are reported at the end of the table.

For robust and comprehensive results, these constraints were obtained using our baseline dataset combined separately with each of the three Type-Ia SNe samples (PantheonPlus, DESY5, and Union3). Thus, in the discussions to follow, the choice of SNe catalog serves to identify the dataset combination being considered.

A. Model 1: $w(a) = w_0[1 + \sin(1 - a)]$

Table II and Fig. 3 summarize the observational constraints on this dark energy model from the three combined analyses described above. Regardless of the choice of SNe sample, the best-fitting $w(a)$ begins in the phantom regime, crosses the phantom divide at $a \simeq 0.7$, and remains in the quintessence regime thereafter.

The mean equation of state parameter, w_0 , deviates from -1 at more than 5σ significance for each dataset combination. However, caution is required when interpreting these results. Since w_0 determines both the present-day value and the phantom crossing of $w(a)$, our constraints on these features are not independent. Furthermore, ΛCDM is not nested within our dark energy models, so the deviation of w_0 from -1 does not represent direct evidence for dynamical dark energy. Nevertheless, the preferred present value and phantom crossing are consistent across the dataset combinations and agree well with the results from the CPL parametrization.

Fig. 3 presents the marginalized 1D and 2D posteriors for the three derived parameters most relevant to cosmological tensions: Ω_m , H_0 , and S_8 . We observe a significant correlation in the w_0 - Ω_m and w_0 - H_0 joint posteriors, in addition to the expected correlation between Ω_m

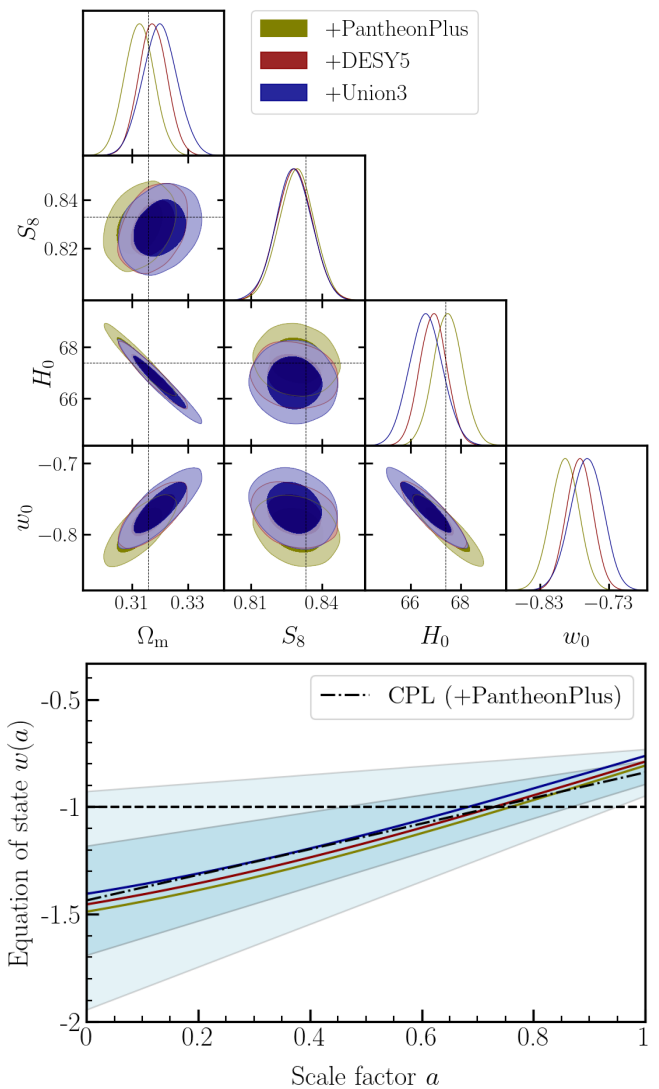


FIG. 3. **Model 1.** Above: Posterior distributions and 1σ , 2σ contours for three key cosmological parameters—the dark energy equation of state parameter w_0 , the Hubble constant H_0 , and the matter fluctuation parameter S_8 —obtained from the combination of our baseline dataset with each of the three Type-Ia SNe samples, as indicated in the legend. The dashed lines represent the mean ΛCDM parameters from *Planck* 2018 [7]. Below: The best-fitting $w(a)$ for the three dataset combinations shown in the legend above. The dash-dot line shows the mean $w(a)$ obtained using the CPL parametrization with the PantheonPlus combination, while the light blue bands indicate the corresponding 1σ and 2σ intervals.

and H_0 . These correlations lead to small shifts in the mean Ω_m and H_0 from their *Planck* 2018 ΛCDM values, with H_0 increasing when using PantheonPlus and decreasing when using the DESY5 or Union3 samples.

To evaluate the improvement of this model over ΛCDM and the CPL parametrization, we use the metrics described in the previous section: the change in the minimum chi-squared, $\Delta\chi^2_{min}$, and the logarithmic Bayes ra-

Parameter	+PantheonPlus	+DESY5	+Union3
$\Omega_c h^2$	0.12056 ± 0.00073	0.12026 ± 0.00074	0.11977 ± 0.00080
$\Omega_b h^2$	0.02233 ± 0.00013	0.02235 ± 0.00013	0.02240 ± 0.00013
$100\theta_{MC}$	1.04085 ± 0.00028	1.04088 ± 0.00029	1.04095 ± 0.00029
τ_{reio}	0.0503 ± 0.0070	0.0517 ± 0.0069	0.0534 ± 0.0070
n_s	0.9640 ± 0.0035	0.9648 ± 0.0034	0.9661 ± 0.0036
$\log(10^{10} A_s)$	3.036 ± 0.013	3.038 ± 0.013	3.041 ± 0.013
w_0	-0.697 ± 0.021	-0.679 ± 0.019	-0.646 ± 0.023
Ω_m	0.3191 ± 0.0055	0.3236 ± 0.0054	0.3320 ± 0.0063
σ_8	0.8158 ± 0.0086	0.8097 ± 0.0083	0.7985 ± 0.0094
S_8	0.8413 ± 0.0076	0.8409 ± 0.0076	0.8399 ± 0.0078
H_0	67.07 ± 0.59	66.54 ± 0.56	65.60 ± 0.66
τ_{drag}	147.00 ± 0.20	147.06 ± 0.20	147.14 ± 0.21
$\Delta\chi^2_{\min} (\Delta \ln B) \Lambda\text{CDM}$	5.1 (−6.5)	−13.1 (2.3)	−13.2 (3.2)
$\Delta\chi^2_{\min} (\Delta \ln B) \text{CPL}$	14.2 (−4.6)	5.7 (−1.3)	0.4 (1.1)

TABLE III. **Model 2.** Constraints (68% CL) on the seven free parameters listed in Table I, along with relevant derived parameters, obtained using the combination of our baseline dataset with each of the three Type-Ia SNe samples (PantheonPlus, DESY5, and Union3) separately. The minimum chi-squared difference, $\Delta\chi^2_{\min}$ [Eq. (9)], and the logarithmic Bayesian evidence ratio, $\Delta \ln B$ [Eq. (10)], are reported at the end of the table.

tio, $\Delta \ln B$. The values of these metrics for Model 1 are consistent with the fact that this model reproduces the $w(a)$ preferred by the CPL parametrization using one fewer parameter: the chi-squared difference from CPL is near zero, while the Bayesian evidence ratios are between 1–2 (Table VI). Hence, the model provides a similar improvement over ΛCDM as does the CPL parametrization.

B. Model 2: $w(a) = w_0 \left[1 + \frac{1-a}{a^2 + (1-a)^2} \right]$

Table III and Fig. 4 summarize the observational constraints. For all three SNe catalogs, the best-fitting $w(a)$ has a phantom crossing at $a \simeq 0.7$, consistent with the previous model. Again, the posterior distribution of the equation of state parameter shows a preference for $w_0 > -1$ at greater than 5σ significance.

The posterior distributions of Ω_m , H_0 , and S_8 are consistent with the *Planck* 2018 ΛCDM results [7] within 68% CL only when PantheonPlus or DESY5 are used. The mean values obtained for H_0 and Ω_m with the Union3 dataset deviate from the mean *Planck* 2018 ΛCDM parameters at approximately 2σ significance. This is likely related to the geometrical degeneracy in the w_0 – Ω_m and w_0 – H_0 planes and the differing Ω_m preferences of the SNe samples. The highest mean value of the Hubble constant, $H_0 = 67.07 \pm 0.59 \text{ km s}^{-1} \text{ Mpc}^{-1}$ (68% CL), is obtained using the PantheonPlus dataset and is slightly below the canonical *Planck* 2018 ΛCDM value.

The model preference statistics at the end of Table III strongly depend on the choice of SNe sample. While both the chi-squared and Bayesian evidence favor this model

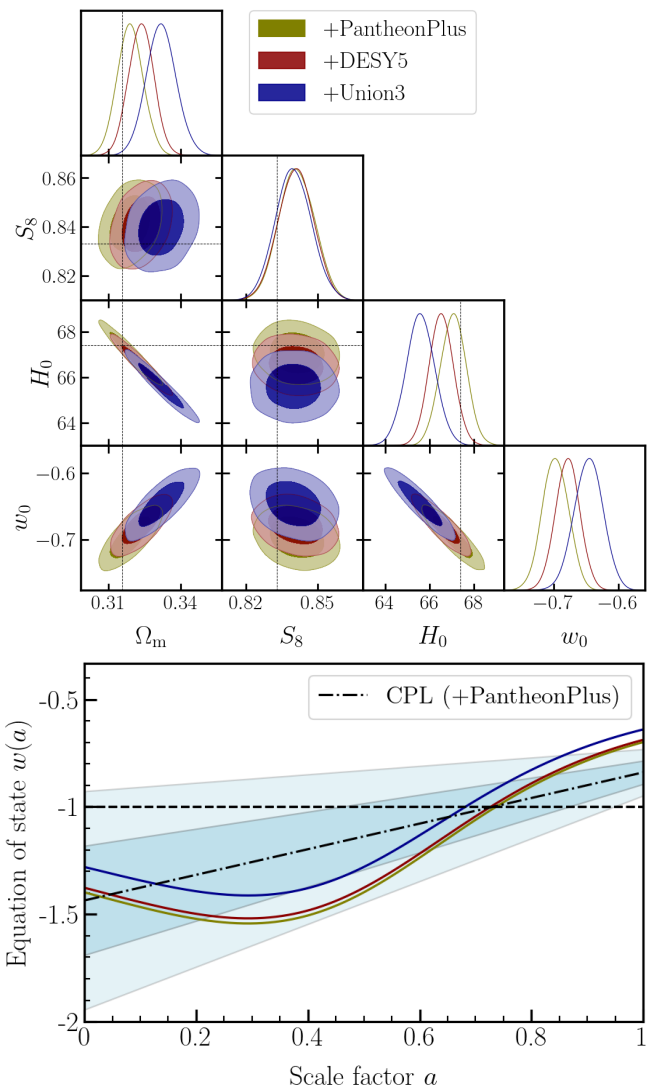


FIG. 4. **Model 2.** *Above:* Posterior distributions and 1σ , 2σ contours for three key cosmological parameters—the dark energy equation of state parameter w_0 , the Hubble constant H_0 , and the matter fluctuation parameter S_8 —obtained from the combination of our baseline dataset with each of the three Type-Ia SNe samples, separately, as indicated in the legend. The dashed lines represent the mean ΛCDM parameter values from *Planck* 2018 [7]. *Below:* The best-fitting $w(a)$ for the three dataset combinations shown in the legend above. The dash-dot line shows the mean $w(a)$ obtained using the CPL parametrization with the PantheonPlus combination, while the light blue bands represent the corresponding 1σ and 2σ intervals.

over ΛCDM when DESY5 or Union3 data are used, PantheonPlus yields $\Delta\chi^2_{\min} \simeq 5$ and $\Delta \ln B \simeq -6.5$, indicating strong support for ΛCDM . This latter dataset also strongly disfavors Model 2 when compared to the CPL parametrization—the only case where this occurs (Table VI and Fig. 8)—while the other two dataset combinations remain mostly agnostic. These weakened preferences are perhaps due to this equation of state’s unusual

Parameter	PantheonPlus	DESY5	Union3
$\Omega_c h^2$	0.11969 ± 0.00072	0.11937 ± 0.00072	0.11925 ± 0.00078
$\Omega_b h^2$	0.02240 ± 0.00013	0.02242 ± 0.00013	0.02243 ± 0.00013
$100\theta_{MC}$	1.04097 ± 0.00028	1.04099 ± 0.00028	1.04101 ± 0.00028
τ_{reio}	0.0538 ± 0.0070	0.0547 ± 0.0069	0.0553 ± 0.0071
n_s	0.9662 ± 0.0034	0.9669 ± 0.0035	0.9674 ± 0.0035
$\log(10^{10} A_s)$	3.042 ± 0.013	3.044 ± 0.013	3.045 ± 0.013
w_0	-0.862 ± 0.023	-0.839 ± 0.021	$-0.829_{-0.025}^{+0.028}$
Ω_m	0.3123 ± 0.0052	0.3169 ± 0.0053	0.3192 ± 0.0062
σ_8	0.8157 ± 0.0086	0.8088 ± 0.0082	0.8059 ± 0.0094
S_8	0.8321 ± 0.0075	0.8313 ± 0.0076	0.8312 ± 0.0077
H_0	67.62 ± 0.58	67.05 ± 0.56	66.78 ± 0.68
τ_{drag}	147.15 ± 0.20	147.21 ± 0.20	147.23 ± 0.21
$\Delta\chi^2_{\min} (\Delta \ln B) \Lambda\text{CDM}$	-10.6 (1.2)	-19.4 (6.0)	-14.0 (3.7)
$\Delta\chi^2_{\min} (\Delta \ln B) \text{CPL}$	-1.5 (3.0)	-0.5 (2.4)	-0.4 (1.6)

TABLE IV. **Model 3.** Constraints (68% CL) on the seven free parameters listed in Table I, alongside relevant derived parameters, using the combination of our baseline dataset with each of the three Type-Ia SNe samples (PantheonPlus, DESY5, and Union3) separately. The minimum chi-squared difference, $\Delta\chi^2_{\min}$ [Eq. (9)], and the logarithmic Bayesian evidence ratio, $\Delta \ln B$ [Eq. (10)], are reported at the end of the table.

shape. To match the phantom crossing preferred by the CPL parametrization, it must deviate from CPL near $a = 1$ at approximately 2σ significance (see the lower panel of Fig. 4).

C. Model 3: $w(a) = w_0 [1 - a \sin(\frac{1}{a}) + \sin 1]$

Table IV and Fig. 5 summarize the observational constraints. This $w(a)$ oscillates with decreasing frequency and increasing amplitude over cosmic time. Most of its oscillations occur within $a \lesssim 0.2$, after which the equation of state evolves monotonically. The best-fitting $w(a)$ closely matches the CPL parametrization for $a \gtrsim 0.5$, suggesting that the early-time oscillations may not significantly affect the preferred value of w_0 . Similar to the previous models, there is a phantom crossing at $a \simeq 0.7$, and the present value of $w(a)$ deviates from -1 at high significance for each dataset combination.

The posterior distributions of the three derived parameters in Fig. 5 (Ω_m , H_0 , and S_8) show qualitative similarities to those of Model 1. The w_0 parameter remains strongly correlated with Ω_m and H_0 , and the mean values of all three parameters are slightly shifted but remain well within 1σ of the *Planck* 2018 ΛCDM results [7].

The model comparison metrics for this model are also qualitatively similar to those of Model 1 (Table VI and Fig. 8), providing a similar improvement over ΛCDM to the CPL parametrization. However, this model improves over Model 1 in fitting the dataset involving PantheonPlus. Using this dataset, the Bayesian evidence for Model 3 compared to CPL becomes moderate ($\Delta \ln B \simeq 3$). Although this improvement could arise

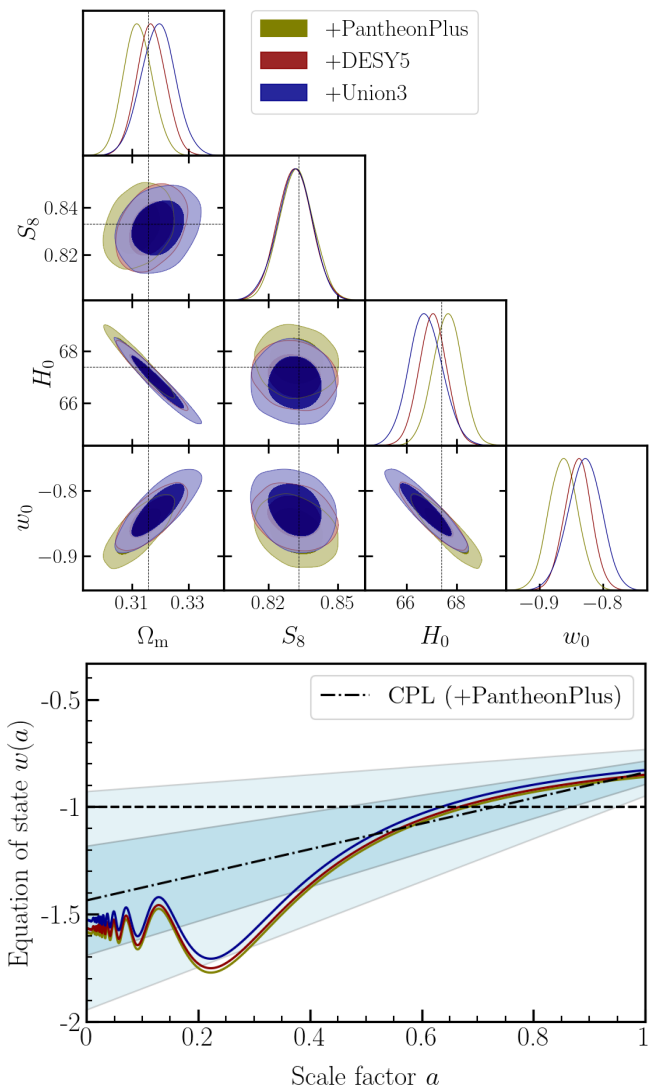


FIG. 5. **Model 3.** Above: Posterior distributions and 1σ , 2σ contours for three key cosmological parameters—the dark energy equation of state parameter w_0 , the Hubble constant H_0 , and the matter fluctuation parameter S_8 —obtained from the combination of our baseline dataset with each of the three Type-Ia SNe samples, separately, as indicated in the legend. The dashed lines represent the mean ΛCDM parameters from *Planck* 2018 [7]. Below: The best-fitting $w(a)$ for the three dataset combinations shown in the legend above. The dash-dot line shows the mean $w(a)$ obtained using the CPL parametrization with the PantheonPlus combination, while the light blue bands represent the corresponding 1σ and 2σ intervals.

from the differences between Models 1 and 3 during late times (for example, the slightly earlier phantom crossing of Model 3), an intriguing possibility is that the markedly different early-time behavior of Model 3 has beneficial downstream effects for fitting the SNe distance measurements.

Parameter	PantheonPlus	DESY5	Union3
$\Omega_c h^2$	0.12008 ± 0.00072	0.11984 ± 0.00074	0.11973 ± 0.00075
$\Omega_b h^2$	0.02237 ± 0.00013	0.02239 ± 0.00013	0.02240 ± 0.00013
$100\theta_{\text{MC}}$	1.04091 ± 0.00028	1.04094 ± 0.00029	1.04095 ± 0.00028
τ_{reio}	0.0524 ± 0.0068	0.0532 ± 0.0069	0.0539 ± 0.0070
n_s	0.9652 ± 0.0035	0.9657 ± 0.0034	0.9662 ± 0.0034
$\log(10^{10} A_s)$	3.039 ± 0.012	3.041 ± 0.013	3.042 ± 0.013
w_0	-0.940 ± 0.026	-0.918 ± 0.024	-0.906 ± 0.031
Ω_m	0.3128 ± 0.0055	0.3169 ± 0.0051	0.3194 ± 0.0064
σ_8	0.8179 ± 0.0084	0.8124 ± 0.0083	0.8093 ± 0.0097
S_8	0.8350 ± 0.0074	0.8349 ± 0.0077	0.8350 ± 0.0075
H_0	67.65 ± 0.60	67.15 ± 0.54	66.87 ± 0.71
τ_{drag}	147.08 ± 0.20	147.13 ± 0.20	147.14 ± 0.20
$\Delta\chi^2_{\text{min}} (\Delta \ln B) \Lambda\text{CDM}$	-12.6 (2.7)	-15.8 (3.9)	-12.7 (2.7)
$\Delta\chi^2_{\text{min}} (\Delta \ln B) \text{CPL}$	-3.5 (4.6)	3.1 (0.3)	0.9 (0.6)

TABLE V. **Model 4.** Constraints (68% CL) on the seven free parameters listed in Table I, alongside relevant derived parameters, obtained using the combination of our baseline dataset with each of the three Type-Ia SNe samples (PantheonPlus, DESY5, and Union3) separately. The minimum chi-squared difference, $\Delta\chi^2_{\text{min}}$ [Eq. (9)], and the logarithmic Bayesian evidence ratio, $\Delta \ln B$ [Eq. (10)], are reported at the end of the table.

D. Model 4: $w(a) = w_0 \left[1 + (1 - a) \sin \left(\frac{1}{1-a} \right) \right]$

Table V and Fig. 6 summarize the observational constraints. The $w(a)$ of this model oscillates with *increasing* frequency and an amplitude that *decreases* over cosmic time, reaching zero at the present day.⁸ The late-time behavior of the best-fitting $w(a)$ is remarkably consistent across the dataset combinations, featuring a phantom crossing at $a \simeq 2/3$ and a present value of $w(a)$ that differs from -1 at approximately 3σ significance. This represents the smallest deviation from -1 among the four models considered. Although one could interpret this as suggestive evidence for present-day oscillations near the cosmological constant, such oscillations are not the only distinctive feature of this model. For instance, the equation of state also has a well-defined peak at $a \simeq 0.78$, regardless of the value of w_0 (Fig. 2). For the best-fitting values of w_0 , this peak rises above the 2σ contour of the CPL parametrization (Fig. 6) and leads to a similar deviation in energy density, $\rho_{\text{DE}}(a)$ (Fig. 7).

Even though this model has a mean w_0 much closer to -1 than the previous three models, the posterior distributions of Ω_m , H_0 , and S_8 are similar. The Hubble constant is again slightly higher when PantheonPlus is used, but for every dataset combination considered, the

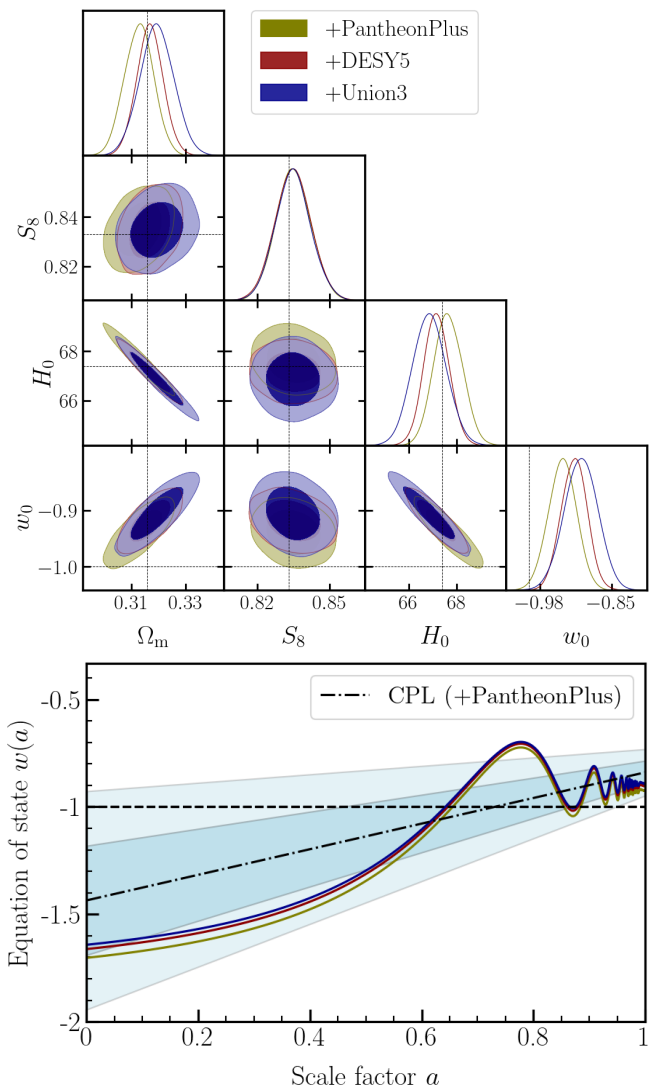


FIG. 6. **Model 4.** Above: Posterior distributions and 1σ , 2σ contours for three key cosmological parameters—the dark energy equation of state parameter w_0 , the Hubble constant H_0 , and the matter fluctuation parameter S_8 —obtained from the combination of our baseline dataset with each of the three Type-Ia SNe samples, separately, as indicated in the legend. The dashed lines represent the mean ΛCDM parameter values from *Planck* 2018 [7]. Below: The best-fitting $w(a)$ for the three dataset combinations shown in the legend above. The dash-dot line shows the mean $w(a)$ obtained using the CPL parametrization with the PantheonPlus combination, while the light blue bands indicate the corresponding 1σ and 2σ intervals.

mean values of these derived parameters are consistent with *Planck* 2018 ΛCDM [7] to within 68% CL.

The model comparison metrics in Table V show that Model 4 is favored over ΛCDM by both of our statistical metrics for every dataset combination considered. In particular, this model provides a significantly better fit to the dataset involving PantheonPlus than Models 1–3 and the CPL parametrization (Table VI and Fig. 8),

⁸ After the present epoch ($a = 1$), the equation of state follows a time-reversed evolution, with oscillations decreasing in frequency and increasing in amplitude. Thus, while $w(a)$ can be extended indefinitely into the future without diverging, the special role assigned to the present day is unjustified. This model should therefore be viewed as a phenomenological framework that allows for present-day oscillations within a generally increasing trend.

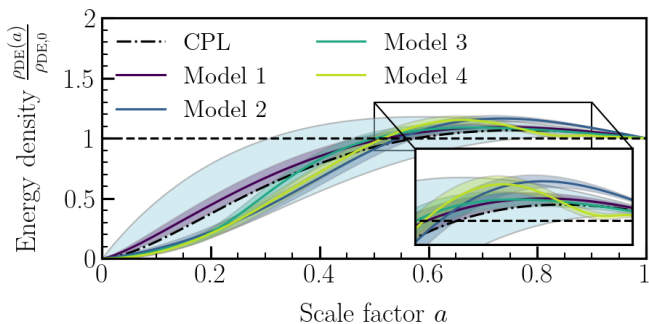


FIG. 7. The mean energy density, $\rho_{\text{DE}}(a)$, and 1σ bands for the CPL parametrization (light blue) and Models 1–4 (colors indicated in the legend), obtained using the dataset combination involving PantheonPlus SNe. Model 4 is notable for its well-defined peak near $a \simeq 2/3$.

achieving $\Delta\chi_{\text{min}}^2 \simeq -3.5$ and $\Delta \ln B \simeq 4.6$ compared to CPL. However, the model also provides a significantly worse fit to the dataset involving DESY5 than Models 1 and 3, although its performance is comparable to CPL in terms of Bayesian evidence. Every model considered, including Model 2, provides a comparable fit to the Union3 dataset.

Regarding the preference of the PantheonPlus dataset for Model 4, and the preference of the DESY5 dataset for models with more linear late-time evolution, one explanation lies in the behavior of $w(a)$ near $a \simeq 2/3$ (redshift $z \simeq 0.5$). Recent non-parametric reconstructions [119–121, 186, 187] have found deviations from Λ CDM in various cosmological functions, including $w(a)$, near this characteristic time. In particular, Refs. [119, 120] demonstrated that the deviation in $w(a)$ near $a \simeq 2/3$ is more pronounced when the DESI BAO data are combined with PantheonPlus than with the DESY5 sample. Our results support these findings within the parametric approach.

V. SUMMARY AND CONCLUSIONS

In this article, we have examined four dynamical dark energy models [Eqs. (5)–(8)], each with a single free parameter, w_0 , that controls both the present-day value and the shape of the dark energy equation of state, $w(a)$. All of these equations of state remain well-defined and contain some oscillations over the full history of the universe, in contrast to the commonly assumed CPL parametrization, which diverges in the infinite future ($a \rightarrow \infty$) and cannot capture deviations from linearity. Unlike the CPL parametrization, which arises from the series expansion of a general $w(a)$ to linear order, our models are purely phenomenological, representing minimal extensions of the Λ CDM model that allow for a dark energy equation of state that broadly increases from the beginning of the universe until the present day. Our main objective was to assess whether any of these models can provide a better fit to modern cosmological data, as mea-

Parameter	PantheonPlus	DESY5	Union3
CPL			
$\Delta\chi_{\text{min}}^2 (\Delta \ln B) \Lambda\text{CDM}$	-9.2 (-1.9)	-18.8 (3.6)	-13.6 (2.1)
Model 1			
$\Delta\chi_{\text{min}}^2 (\Delta \ln B) \Lambda\text{CDM}$	-8.2 (-0.0)	-19.3 (5.6)	-12.8 (3.3)
$\Delta\chi_{\text{min}}^2 (\Delta \ln B) \text{CPL}$	1.0 (1.8)	-0.4 (2.1)	0.8 (1.2)
Model 2			
$\Delta\chi_{\text{min}}^2 (\Delta \ln B) \Lambda\text{CDM}$	5.1 (-6.5)	-13.1 (2.3)	-13.2 (3.2)
$\Delta\chi_{\text{min}}^2 (\Delta \ln B) \text{CPL}$	14.2 (-4.6)	5.7 (-1.3)	0.4 (1.1)
Model 3			
$\Delta\chi_{\text{min}}^2 (\Delta \ln B) \Lambda\text{CDM}$	-10.6 (1.2)	-19.4 (6.0)	-14.0 (3.7)
$\Delta\chi_{\text{min}}^2 (\Delta \ln B) \text{CPL}$	-1.5 (3.0)	-0.5 (2.4)	-0.4 (1.6)
Model 4			
$\Delta\chi_{\text{min}}^2 (\Delta \ln B) \Lambda\text{CDM}$	-12.6 (2.7)	-15.8 (3.9)	-12.7 (2.7)
$\Delta\chi_{\text{min}}^2 (\Delta \ln B) \text{CPL}$	-3.5 (4.6)	3.1 (0.3)	0.9 (0.6)

TABLE VI. A summary of model preference statistics—the minimum chi-squared difference, $\Delta\chi_{\text{min}}^2$ [Eq. (9)], and the logarithmic Bayesian evidence ratio, $\Delta \ln B$ [Eq. (10)]—for the CPL parametrization and the one-parameter models considered in this work. A preference for Models 1–4 is theoretically indicated by $\Delta\chi_{\text{min}}^2 > 0$ and $\Delta \ln B > 0$, while $\Delta\chi_{\text{min}}^2 < 0$ and $\Delta \ln B < 0$ indicate a preference for the reference models. More precise benchmarks for $\Delta \ln B$ are provided by the revised Jeffreys’ scale (Section III A).

sured by the chi-squared statistic and Bayesian evidence, than the CPL parametrization.

Among the four models considered, only one evolves monotonically over the time domain $a \in [0, 1]$ that is relevant to our analysis. One other model has a single “oscillation,” decreasing until $a \simeq 0.3$ and increasing thereafter. The remaining two models exhibit rapid oscillations either toward the beginning of the universe ($a = 0$) or the present day ($a = 1$). The latter Model 4 is particularly noteworthy, as it simultaneously captures the increasing trend suggested by previous studies (e.g., those by DESI [124, 125, 133, 135]) and the late-time oscillations identified in non-parametric reconstructions [115–117, 119–121, 170]. To our knowledge, this model has not been previously considered in the literature.

These models were analyzed using a combination of CMB data from *Planck*, lensing reconstruction from ACT-DR6, BAO measurements from DESI-DR2, and three separate Type-Ia Supernovae samples: PantheonPlus, DESY5, and Union3. The resulting parameter constraints are presented in Tables II–V and Figs. 3–6. Each best-fitting $w(a)$ has a present-day value greater than -1 at several standard deviations and a phantom crossing near $a \simeq 0.6$ – 0.7 . This behavior is qualitatively consistent with both the CPL parametrization and non-parametric reconstruction results from DESI [124, 125, 133, 135].

Our main results regarding model preferences—measured by the minimum chi-squared difference, $\Delta\chi_{\text{min}}^2$

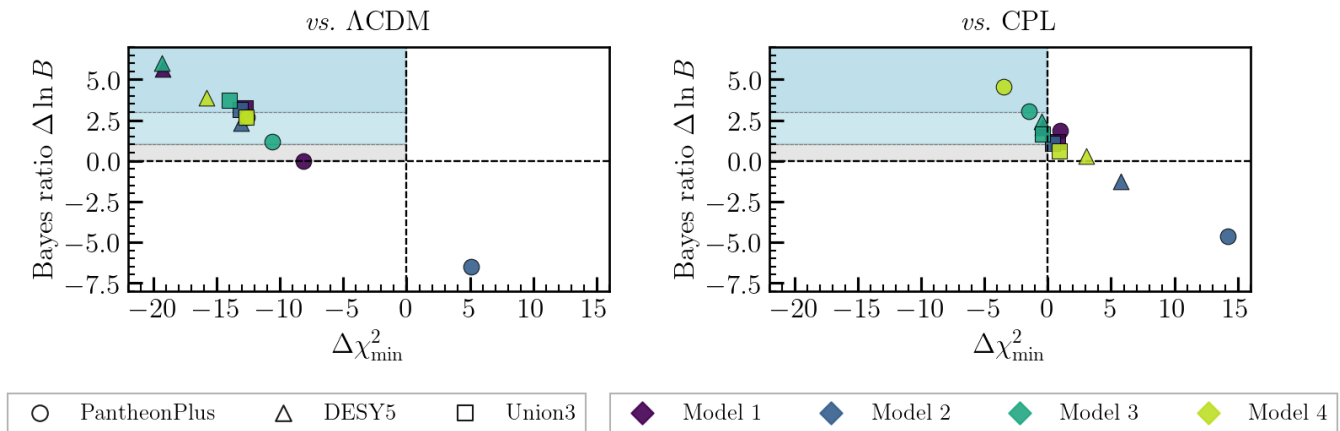


FIG. 8. A summary of the datasets’ model preferences, as quantified by the change in the minimum chi-squared, $\Delta\chi^2_{\min}$ [Eq. (9)], and the logarithmic Bayes ratio, $\Delta \ln B$ [Eq. (10)], for each one-parameter model in Eqs. (5)–(8). The dataset combinations are defined by the Type-Ia SNe sample (PantheonPlus, DESY5, or Union3) used alongside our baseline (Section III). The top-left quadrants indicate preference for our models, and the shaded bands demarcate the revised Jeffreys’ scale (Section III A). Compared to Λ CDM (*Left*), all models except Model 2 with PantheonPlus SNe are significantly favored by one or both statistics. Versus the CPL parametrization (*Right*), Model 4 combined with PantheonPlus SNe provides the most significant improvement.

[Eq. (9)], and logarithmic Bayes ratio, $\Delta \ln B$ [Eq. (10)]—for our one-parameter models compared to Λ CDM and the CPL parametrization are shown in Fig. 8 and Table VI. These results can be summarized as follows:

- All datasets significantly prefer the one-parameter models over Λ CDM according to the chi-squared statistic, with the exception of Model 2 and the dataset involving PantheonPlus, which is significantly disfavored. The DESY5 dataset provides the highest Bayesian evidence ($\Delta \ln B \simeq 5$) for Models 1 and 3, whereas the Union3 dataset provides similar levels of support for each model.
- Model 4 with PantheonPlus is significantly favored over the CPL parametrization by the Bayesian evidence, with $\Delta \ln B \simeq 4.5$. Using the same dataset, Model 3 is moderately favored ($\Delta \ln B \simeq 3$). All other datasets are either indecisive or favor the CPL parametrization over the one-parameter models.
- The strong preference for Model 4 from PantheonPlus is possibly explained by this model’s $w(a)$ having a well-defined peak near $a \simeq 0.78$, leading to a similar peak in $\rho_{\text{DE}}(a)$ near $a \simeq 2/3$ (Fig. 7). Such features were also found near this scale factor in non-parametric reconstructions of $w(a)$ using PantheonPlus SNe (less so with DESY5) [119, 120].

In conclusion, we have identified several one-parameter models of dark energy that are preferred over Λ CDM and the CPL parametrization by standard statistical metrics, depending on the SNe catalog used in the analysis. Our results add to the growing collection of evidence for deviations from Λ CDM near $a \simeq 2/3$ ($z \simeq 0.5$) [119–121, 186, 187], motivating further studies on dark energy models with late-time oscillations.

VI. ACKNOWLEDGMENTS

We thank William Giarè for the interesting and useful discussions and for his contribution in developing the Cobaya wrapper for the MCEvidence. SP acknowledges the financial support from the Department of Science and Technology (DST), Govt. of India under the Scheme “Fund for Improvement of S&T Infrastructure (FIST)” [File No. SR/FST/MS-I/2019/41]. EDV is supported by a Royal Society Dorothy Hodgkin Research Fellowship. This article is based upon work from the COST Action CA21136 “Addressing observational tensions in cosmology with systematics and fundamental physics” (CosmoVerse), supported by COST (European Cooperation in Science and Technology). We acknowledge IT Services at The University of Sheffield for the provision of services for High Performance Computing.

[1] A. G. Riess *et al.* (Supernova Search Team), Observational evidence from supernovae for an accelerating universe and a cosmological constant, *Astron. J.* **116**, 1009 (1998), [arXiv:astro-ph/9805201](#).

[2] S. Perlmutter *et al.* (Supernova Cosmology Project), Measurements of Ω and Λ from 42 High Redshift Supernovae, *Astrophys. J.* **517**, 565 (1999), [arXiv:astro-ph/9812133](#).

- [3] S. Weinberg, The Cosmological Constant Problem, *Rev. Mod. Phys.* **61**, 1 (1989).
- [4] I. Zlatev, L.-M. Wang, and P. J. Steinhardt, Quintessence, cosmic coincidence, and the cosmological constant, *Phys. Rev. Lett.* **82**, 896 (1999), [arXiv:astro-ph/9807002](#).
- [5] A. Joyce, B. Jain, J. Khoury, and M. Trodden, Beyond the Cosmological Standard Model, *Phys. Rept.* **568**, 1 (2015), [arXiv:1407.0059 \[astro-ph.CO\]](#).
- [6] P. Bull *et al.*, Beyond Λ CDM: Problems, solutions, and the road ahead, *Phys. Dark Univ.* **12**, 56 (2016), [arXiv:1512.05356 \[astro-ph.CO\]](#).
- [7] N. Aghanim *et al.* (Planck), Planck 2018 results. VI. Cosmological parameters, *Astron. Astrophys.* **641**, A6 (2020), [Erratum: *Astron. Astrophys.* 652, C4 (2021)], [arXiv:1807.06209 \[astro-ph.CO\]](#).
- [8] A. G. Riess *et al.*, A Comprehensive Measurement of the Local Value of the Hubble Constant with 1 km s⁻¹ Mpc⁻¹ Uncertainty from the Hubble Space Telescope and the SH0ES Team, *Astrophys. J. Lett.* **934**, L7 (2022), [arXiv:2112.04510 \[astro-ph.CO\]](#).
- [9] Y. S. Murakami, A. G. Riess, B. E. Stahl, W. D. Kenworthy, D.-M. A. Pluck, A. Macoreta, D. Brout, D. O. Jones, D. M. Scolnic, and A. V. Filippenko, Leveraging SN Ia spectroscopic similarity to improve the measurement of H₀, *JCAP* **11**, 046, [arXiv:2306.00070 \[astro-ph.CO\]](#).
- [10] L. Breuval, A. G. Riess, S. Casertano, W. Yuan, L. M. Macri, M. Romaniello, Y. S. Murakami, D. Scolnic, G. S. Anand, and I. Soszyński, Small Magellanic Cloud Cepheids Observed with the Hubble Space Telescope Provide a New Anchor for the SH0ES Distance Ladder, *Astrophys. J.* **973**, 30 (2024), [arXiv:2404.08038 \[astro-ph.CO\]](#).
- [11] E. Di Valentino *et al.*, Cosmology Intertwined III: $f\sigma_8$ and S_8 , *Astropart. Phys.* **131**, 102604 (2021), [arXiv:2008.11285 \[astro-ph.CO\]](#).
- [12] E. Di Valentino and S. Bridle, Exploring the Tension between Current Cosmic Microwave Background and Cosmic Shear Data, *Symmetry* **10**, 585 (2018).
- [13] A. Amon *et al.* (DES), Dark Energy Survey Year 3 results: Cosmology from cosmic shear and robustness to data calibration, *Phys. Rev. D* **105**, 023514 (2022), [arXiv:2105.13543 \[astro-ph.CO\]](#).
- [14] L. F. Secco *et al.* (DES), Dark Energy Survey Year 3 results: Cosmology from cosmic shear and robustness to modeling uncertainty, *Phys. Rev. D* **105**, 023515 (2022), [arXiv:2105.13544 \[astro-ph.CO\]](#).
- [15] M. Asgari *et al.* (KiDS), KiDS-1000 Cosmology: Cosmic shear constraints and comparison between two point statistics, *Astron. Astrophys.* **645**, A104 (2021), [arXiv:2007.15633 \[astro-ph.CO\]](#).
- [16] M. Asgari *et al.*, KiDS+VIKING-450 and DES-Y1 combined: Mitigating baryon feedback uncertainty with COSEBIs, *Astron. Astrophys.* **634**, A127 (2020), [arXiv:1910.05336 \[astro-ph.CO\]](#).
- [17] S. Joudaki *et al.*, KiDS+VIKING-450 and DES-Y1 combined: Cosmology with cosmic shear, *Astron. Astrophys.* **638**, L1 (2020), [arXiv:1906.09262 \[astro-ph.CO\]](#).
- [18] G. D'Amico, J. Gleyzes, N. Kokron, K. Markovic, L. Senatore, P. Zhang, F. Beutler, and H. Gil-Marín, The Cosmological Analysis of the SDSS/BOSS data from the Effective Field Theory of Large-Scale Structure, *JCAP* **05**, 005, [arXiv:1909.05271 \[astro-ph.CO\]](#).
- [19] T. M. C. Abbott *et al.* (Kilo-Degree Survey, DES), DES Y3 + KiDS-1000: Consistent cosmology combining cosmic shear surveys, *Open J. Astrophys.* **6**, 2305.17173 (2023), [arXiv:2305.17173 \[astro-ph.CO\]](#).
- [20] T. Tröster *et al.*, Cosmology from large-scale structure: Constraining Λ CDM with BOSS, *Astron. Astrophys.* **633**, L10 (2020), [arXiv:1909.11006 \[astro-ph.CO\]](#).
- [21] C. Heymans *et al.*, KiDS-1000 Cosmology: Multi-probe weak gravitational lensing and spectroscopic galaxy clustering constraints, *Astron. Astrophys.* **646**, A140 (2021), [arXiv:2007.15632 \[astro-ph.CO\]](#).
- [22] R. Dalal *et al.*, Hyper Suprime-Cam Year 3 results: Cosmology from cosmic shear power spectra, *Phys. Rev. D* **108**, 123519 (2023), [arXiv:2304.00701 \[astro-ph.CO\]](#).
- [23] S. Chen *et al.*, Not all lensing is low: An analysis of DESI×DES using the Lagrangian Effective Theory of LSS (2024), [arXiv:2407.04795 \[astro-ph.CO\]](#).
- [24] J. Kim *et al.* (ACT, DESI), The Atacama Cosmology Telescope DR6 and DESI: Structure formation over cosmic time with a measurement of the cross-correlation of CMB Lensing and Luminous Red Galaxies (2024), [arXiv:2407.04606 \[astro-ph.CO\]](#).
- [25] L. Faga *et al.* (DES), Dark Energy Survey Year 3 Results: Cosmology from galaxy clustering and galaxy-galaxy lensing in harmonic space (2024), [arXiv:2406.12675 \[astro-ph.CO\]](#).
- [26] J. Harnois-Deraps *et al.*, KiDS-1000 and DES-Y1 combined: Cosmology from peak count statistics (2024), [arXiv:2405.10312 \[astro-ph.CO\]](#).
- [27] A. Dvornik *et al.*, KiDS-1000: Combined halo-model cosmology constraints from galaxy abundance, galaxy clustering and galaxy-galaxy lensing, *Astron. Astrophys.* **675**, A189 (2023), [arXiv:2210.03110 \[astro-ph.CO\]](#).
- [28] T. M. C. Abbott *et al.* (DES), Dark Energy Survey Year 3 results: Cosmological constraints from galaxy clustering and weak lensing, *Phys. Rev. D* **105**, 023520 (2022), [arXiv:2105.13549 \[astro-ph.CO\]](#).
- [29] A. H. Wright *et al.*, KiDS-Legacy: Cosmological constraints from cosmic shear with the complete Kilo-Degree Survey (2025), [arXiv:2503.19441 \[astro-ph.CO\]](#).
- [30] E. Di Valentino, O. Mena, S. Pan, L. Visinelli, W. Yang, A. Melchiorri, D. F. Mota, A. G. Riess, and J. Silk, In the realm of the Hubble tension—a review of solutions, *Class. Quant. Grav.* **38**, 153001 (2021), [arXiv:2103.01183 \[astro-ph.CO\]](#).
- [31] E. Abdalla *et al.*, Cosmology intertwined: A review of the particle physics, astrophysics, and cosmology associated with the cosmological tensions and anomalies, *JHEAp* **34**, 49 (2022), [arXiv:2203.06142 \[astro-ph.CO\]](#).
- [32] L. Perivolaropoulos and F. Skara, Challenges for Λ CDM: An update, *New Astron. Rev.* **95**, 101659 (2022), [arXiv:2105.05208 \[astro-ph.CO\]](#).
- [33] A. R. Khalife, M. B. Zanjani, S. Galli, S. Günther, J. Lesgourgues, and K. Benabed, Review of Hubble tension solutions with new SH0ES and SPT-3G data, *JCAP* **04**, 059, [arXiv:2312.09814 \[astro-ph.CO\]](#).
- [34] E. Di Valentino and D. Brout, eds., *The Hubble Constant Tension*, Springer Series in Astrophysics and Cosmology (Springer, 2024).
- [35] A. R. Cooray and D. Huterer, Gravitational lensing as a probe of quintessence, *Astrophys. J. Lett.* **513**, L95 (1999), [arXiv:astro-ph/9901097](#).

- [36] G. Efstathiou, Constraining the equation of state of the universe from distant type Ia supernovae and cosmic microwave background anisotropies, *Mon. Not. Roy. Astron. Soc.* **310**, 842 (1999), [arXiv:astro-ph/9904356](#).
- [37] P. Astier, Can luminosity distance measurements probe the equation of state of dark energy, *Phys. Lett. B* **500**, 8 (2001), [arXiv:astro-ph/0008306](#).
- [38] J. Weller and A. Albrecht, Future supernovae observations as a probe of dark energy, *Phys. Rev. D* **65**, 103512 (2002), [arXiv:astro-ph/0106079](#).
- [39] P. S. Corasaniti and E. J. Copeland, A Model independent approach to the dark energy equation of state, *Phys. Rev. D* **67**, 063521 (2003), [arXiv:astro-ph/0205544](#).
- [40] C. Wetterich, Phenomenological parameterization of quintessence, *Phys. Lett. B* **594**, 17 (2004), [arXiv:astro-ph/0403289](#).
- [41] B. A. Bassett, P. S. Corasaniti, and M. Kunz, The Essence of quintessence and the cost of compression, *Astrophys. J. Lett.* **617**, L1 (2004), [arXiv:astro-ph/0407364](#).
- [42] B. Feng, M. Li, Y.-S. Piao, and X. Zhang, Oscillating quintom and the recurrent universe, *Phys. Lett. B* **634**, 101 (2006), [arXiv:astro-ph/0407432](#).
- [43] S. Hannestad and E. Mortsell, Cosmological constraints on the dark energy equation of state and its evolution, *JCAP* **09**, 001, [arXiv:astro-ph/0407259](#).
- [44] J.-Q. Xia, B. Feng, and X.-M. Zhang, Constraints on oscillating quintom from supernova, microwave background and galaxy clustering, *Mod. Phys. Lett. A* **20**, 2409 (2005), [arXiv:astro-ph/0411501](#).
- [45] U. Alam, V. Sahni, and A. A. Starobinsky, The Case for dynamical dark energy revisited, *JCAP* **06**, 008, [arXiv:astro-ph/0403687](#).
- [46] A. Upadhye, M. Ishak, and P. J. Steinhardt, Dynamical dark energy: Current constraints and forecasts, *Phys. Rev. D* **72**, 063501 (2005), [arXiv:astro-ph/0411803](#).
- [47] Y.-g. Gong and Y.-Z. Zhang, Probing the curvature and dark energy, *Phys. Rev. D* **72**, 043518 (2005), [arXiv:astro-ph/0502262](#).
- [48] H. K. Jassal, J. S. Bagla, and T. Padmanabhan, Observational constraints on low redshift evolution of dark energy: How consistent are different observations?, *Phys. Rev. D* **72**, 103503 (2005), [arXiv:astro-ph/0506748](#).
- [49] S. Nesseris and L. Perivolaropoulos, Comparison of the legacy and gold snia dataset constraints on dark energy models, *Phys. Rev. D* **72**, 123519 (2005), [arXiv:astro-ph/0511040](#).
- [50] K. N. Ananda and M. Bruni, Cosmo-dynamics and dark energy with non-linear equation of state: a quadratic model, *Phys. Rev. D* **74**, 023523 (2006), [arXiv:astro-ph/0512224](#).
- [51] E. V. Linder, On oscillating dark energy, *Astropart. Phys.* **25**, 167 (2006), [arXiv:astro-ph/0511415](#).
- [52] S. Nojiri and S. D. Odintsov, The Oscillating dark energy: Future singularity and coincidence problem, *Phys. Lett. B* **637**, 139 (2006), [arXiv:hep-th/0603062](#).
- [53] D. Jain, A. Dev, and J. S. Alcaniz, Cosmological bounds on oscillating dark energy models, *Phys. Lett. B* **656**, 15 (2007), [arXiv:0709.4234 \[astro-ph\]](#).
- [54] A. Kurek, O. Hrycyna, and M. Szydlowski, Constraints on oscillating dark energy models, *Phys. Lett. B* **659**, 14 (2008), [arXiv:0707.0292 \[astro-ph\]](#).
- [55] K. Ichikawa and T. Takahashi, The Hubble Constant and Dark Energy from Cosmological Distance Measures, *JCAP* **04**, 027, [arXiv:0710.3995 \[astro-ph\]](#).
- [56] D.-J. Liu, X.-Z. Li, J. Hao, and X.-H. Jin, Revisiting the parametrization of Equation of State of Dark Energy via SNIa Data, *Mon. Not. Roy. Astron. Soc.* **388**, 275 (2008), [arXiv:0804.3829 \[astro-ph\]](#).
- [57] E. M. Barboza, Jr. and J. S. Alcaniz, A parametric model for dark energy, *Phys. Lett. B* **666**, 415 (2008), [arXiv:0805.1713 \[astro-ph\]](#).
- [58] E. M. Barboza, J. S. Alcaniz, Z. H. Zhu, and R. Silva, A generalized equation of state for dark energy, *Phys. Rev. D* **80**, 043521 (2009), [arXiv:0905.4052 \[astro-ph.CO\]](#).
- [59] A. Kurek, O. Hrycyna, and M. Szydlowski, From model dynamics to oscillating dark energy parametrisation, *Phys. Lett. B* **690**, 337 (2010), [arXiv:0805.4005 \[astro-ph\]](#).
- [60] J.-Z. Ma and X. Zhang, Probing the dynamics of dark energy with novel parametrizations, *Phys. Lett. B* **699**, 233 (2011), [arXiv:1102.2671 \[astro-ph.CO\]](#).
- [61] I. Sendra and R. Lazkoz, SN and BAO constraints on (new) polynomial dark energy parametrizations: current results and forecasts, *Mon. Not. Roy. Astron. Soc.* **422**, 776 (2012), [arXiv:1105.4943 \[astro-ph.CO\]](#).
- [62] L. Feng and T. Lu, A new equation of state for dark energy model, *JCAP* **11**, 034, [arXiv:1203.1784 \[astro-ph.CO\]](#).
- [63] F. Pace, C. Fedeli, L. Moscardini, and M. Bartelmann, Structure formation in cosmologies with oscillating dark energy, *Mon. Not. Roy. Astron. Soc.* **422**, 1186 (2012), [arXiv:1111.1556 \[astro-ph.CO\]](#).
- [64] E. M. Barboza, Jr. and J. S. Alcaniz, Probing the time dependence of dark energy, *JCAP* **02**, 042, [arXiv:1103.0257 \[astro-ph.CO\]](#).
- [65] A. De Felice, S. Nesseris, and S. Tsujikawa, Observational constraints on dark energy with a fast varying equation of state, *JCAP* **05**, 029, [arXiv:1203.6760 \[astro-ph.CO\]](#).
- [66] C.-J. Feng, X.-Y. Shen, P. Li, and X.-Z. Li, A New Class of Parametrization for Dark Energy without Divergence, *JCAP* **09**, 023, [arXiv:1206.0063 \[astro-ph.CO\]](#).
- [67] H. Wei, X.-P. Yan, and Y.-N. Zhou, Cosmological Applications of Padé Approximant, *JCAP* **01**, 045, [arXiv:1312.1117 \[astro-ph.CO\]](#).
- [68] S. Sello, A general parametric model for the dynamic dark energy (2013), [arXiv:1308.0449 \[astro-ph.CO\]](#).
- [69] J. Magaña, V. H. Cárdenas, and V. Motta, Cosmic slowing down of acceleration for several dark energy parametrizations, *JCAP* **10**, 017, [arXiv:1407.1632 \[astro-ph.CO\]](#).
- [70] O. Akarsu, T. Dereli, and J. A. Vazquez, A divergence-free parametrization for dynamical dark energy, *JCAP* **06**, 049, [arXiv:1501.07598 \[astro-ph.CO\]](#).
- [71] S. Pan, J. de Haro, A. Paliathanasis, and R. J. Slagter, Evolution and Dynamics of a Matter creation model, *Mon. Not. Roy. Astron. Soc.* **460**, 1445 (2016), [arXiv:1601.03955 \[gr-qc\]](#).
- [72] E. Di Valentino, A. Melchiorri, and J. Silk, Reconciling Planck with the local value of H_0 in extended parameter space, *Phys. Lett. B* **761**, 242 (2016), [arXiv:1606.00634 \[astro-ph.CO\]](#).
- [73] R. C. Nunes, A. Bonilla, S. Pan, and E. N. Saridakis, Observational Constraints on $f(T)$ gravity from varying fundamental constants, *Eur. Phys. J. C* **77**, 230 (2017),

- arXiv:1608.01960 [gr-qc].
- [74] R. C. Nunes, S. Pan, E. N. Saridakis, and E. M. C. Abreu, New observational constraints on $f(R)$ gravity from cosmic chronometers, *JCAP* **01**, 005, arXiv:1610.07518 [astro-ph.CO].
- [75] J. Magana, V. Motta, V. H. Cardenas, and G. Foex, Testing cosmic acceleration for $w(z)$ parameterizations using f_{gas} measurements in galaxy clusters, *Mon. Not. Roy. Astron. Soc.* **469**, 47 (2017), arXiv:1703.08521 [astro-ph.CO].
- [76] W. Yang, S. Pan, and A. Paliathanasis, Latest astronomical constraints on some non-linear parametric dark energy models, *Mon. Not. Roy. Astron. Soc.* **475**, 2605 (2018), arXiv:1708.01717 [gr-qc].
- [77] S. Pan, E. N. Saridakis, and W. Yang, Observational Constraints on Oscillating Dark-Energy Parametrizations, *Phys. Rev. D* **98**, 063510 (2018), arXiv:1712.05746 [astro-ph.CO].
- [78] G. Panotopoulos and A. Rincón, Growth index and statefinder diagnostic of Oscillating Dark Energy, *Phys. Rev. D* **97**, 103509 (2018), arXiv:1804.11208 [astro-ph.CO].
- [79] W. Yang, S. Pan, E. Di Valentino, E. N. Saridakis, and S. Chakraborty, Observational constraints on one-parameter dynamical dark-energy parameterizations and the H_0 tension, *Phys. Rev. D* **99**, 043543 (2019), arXiv:1810.05141 [astro-ph.CO].
- [80] L. G. Jaime, M. Jaber, and C. Escamilla-Rivera, New parametrized equation of state for dark energy surveys, *Phys. Rev. D* **98**, 083530 (2018), arXiv:1804.04284 [astro-ph.CO].
- [81] A. Das, A. Banerjee, S. Chakraborty, and S. Pan, Perfect Fluid Cosmological Universes: One equation of state and the most general solution, *Pramana* **90**, 19 (2018), arXiv:1706.08145 [gr-qc].
- [82] W. Yang, S. Pan, E. Di Valentino, and E. N. Saridakis, Observational constraints on dynamical dark energy with pivoting redshift, *Universe* **5**, 219 (2019), arXiv:1811.06932 [astro-ph.CO].
- [83] M. Du, W. Yang, L. Xu, S. Pan, and D. F. Mota, Future constraints on dynamical dark-energy using gravitational-wave standard sirens, *Phys. Rev. D* **100**, 043535 (2019), arXiv:1812.01440 [astro-ph.CO].
- [84] X. Li and A. Shafieloo, A Simple Phenomenological Emergent Dark Energy Model can Resolve the Hubble Tension, *Astrophys. J. Lett.* **883**, L3 (2019), arXiv:1906.08275 [astro-ph.CO].
- [85] W. Yang, S. Pan, A. Paliathanasis, S. Ghosh, and Y. Wu, Observational constraints of a new unified dark fluid and the H_0 tension, *Mon. Not. Roy. Astron. Soc.* **490**, 2071 (2019), arXiv:1904.10436 [gr-qc].
- [86] S. Pan, W. Yang, E. Di Valentino, A. Shafieloo, and S. Chakraborty, Reconciling H_0 tension in a six parameter space?, *JCAP* **06** (06), 062, arXiv:1907.12551 [astro-ph.CO].
- [87] D. Tamayo and J. A. Vazquez, Fourier-series expansion of the dark-energy equation of state, *Mon. Not. Roy. Astron. Soc.* **487**, 729 (2019), arXiv:1901.08679 [astro-ph.CO].
- [88] M. Rezaei, Observational constraints on the oscillating dark energy cosmologies, *Mon. Not. Roy. Astron. Soc.* **485**, 550 (2019), arXiv:1902.04776 [gr-qc].
- [89] S. Pan, W. Yang, and A. Paliathanasis, Imprints of an extended Chevallier–Polarski–Linder parametrization on the large scale of our universe, *Eur. Phys. J. C* **80**, 274 (2020), arXiv:1902.07108 [astro-ph.CO].
- [90] M. Rezaei, T. Naderi, M. Malekjani, and A. Mehrabi, A Bayesian comparison between Λ CDM and phenomenologically emergent dark energy models, *Eur. Phys. J. C* **80**, 374 (2020), arXiv:2004.08168 [astro-ph.CO].
- [91] E. Di Valentino, A. Mukherjee, and A. A. Sen, Dark Energy with Phantom Crossing and the H_0 Tension, *Entropy* **23**, 404 (2021), arXiv:2005.12587 [astro-ph.CO].
- [92] D. Perkovic and H. Stefancic, Barotropic fluid compatible parametrizations of dark energy, *Eur. Phys. J. C* **80**, 629 (2020), arXiv:2004.05342 [gr-qc].
- [93] A. Banihashemi, N. Khosravi, and A. Shafieloo, Dark energy as a critical phenomenon: a hint from Hubble tension, *JCAP* **06**, 003, arXiv:2012.01407 [astro-ph.CO].
- [94] M. Jaber-Bravo, E. Almaraz, and A. de la Macorra, Imprint of a Steep Equation of State in the growth of structure, *Astropart. Phys.* **115**, 102388 (2020), arXiv:1906.09522 [astro-ph.CO].
- [95] H. B. Benaoum, W. Yang, S. Pan, and E. Di Valentino, Modified emergent dark energy and its astronomical constraints, *Int. J. Mod. Phys. D* **31**, 2250015 (2022), arXiv:2008.09098 [gr-qc].
- [96] W. Yang, E. Di Valentino, S. Pan, A. Shafieloo, and X. Li, Generalized emergent dark energy model and the Hubble constant tension, *Phys. Rev. D* **104**, 063521 (2021), arXiv:2103.03815 [astro-ph.CO].
- [97] M. Jaber, G. Arciniega, L. G. Jaime, and O. A. Rodríguez-López, A single parameterization for dark energy and modified gravity models, *Phys. Dark Univ.* **37**, 101069 (2022), arXiv:2102.08561 [astro-ph.CO].
- [98] G. Alestas, D. Camarena, E. Di Valentino, L. Kazantzidis, V. Marra, S. Nesseris, and L. Perivolaropoulos, Late-transition versus smooth $H(z)$ -deformation models for the resolution of the Hubble crisis, *Phys. Rev. D* **105**, 063538 (2022), arXiv:2110.04336 [astro-ph.CO].
- [99] J. Yang, X.-Y. Fan, C.-J. Feng, and X.-H. Zhai, Latest Data Constraint of Some Parameterized Dark Energy Models, *Chin. Phys. Lett.* **40**, 019801 (2023), arXiv:2211.15881 [astro-ph.CO].
- [100] H. G. Escudero, J.-L. Kuo, R. E. Keeley, and K. N. Abazajian, Early or phantom dark energy, self-interacting, extra, or massive neutrinos, primordial magnetic fields, or a curved universe: An exploration of possible solutions to the H_0 and σ_8 problems, *Phys. Rev. D* **106**, 103517 (2022), arXiv:2208.14435 [astro-ph.CO].
- [101] M. N. Castillo-Santos, A. Hernández-Almada, M. A. García-Aspeitia, and J. Magaña, An exponential equation of state of dark energy in the light of 2018 CMB Planck data, *Phys. Dark Univ.* **40**, 101225 (2023), arXiv:2212.01974 [astro-ph.CO].
- [102] W. Yang, W. Giarè, S. Pan, E. Di Valentino, A. Melchiorri, and J. Silk, Revealing the effects of curvature on the cosmological models, *Phys. Rev. D* **107**, 063509 (2023), arXiv:2210.09865 [astro-ph.CO].
- [103] S. Dahmani, A. Bouali, I. El Bojaddaini, A. Errahmani, and T. Ouali, Smoothing the H_0 tension with a phantom dynamical dark energy model, *Phys. Dark Univ.* **42**, 101266 (2023), arXiv:2301.04200 [astro-ph.CO].
- [104] L. A. Escamilla, W. Giarè, E. Di Valentino, R. C. Nunes, and S. Vagnozzi, The state of the dark energy equation

- of state circa 2023, *JCAP* **05**, 091, [arXiv:2307.14802 \[astro-ph.CO\]](#).
- [105] M. Rezaei, S. Pan, W. Yang, and D. F. Mota, Evidence of dynamical dark energy in a non-flat universe: current and future observations, *JCAP* **01**, 052, [arXiv:2305.18544 \[astro-ph.CO\]](#).
- [106] S. A. Adil, O. Akarsu, E. Di Valentino, R. C. Nunes, E. Özülker, A. A. Sen, and E. Specogna, Omnipotent dark energy: A phenomenological answer to the Hubble tension, *Phys. Rev. D* **109**, 023527 (2024), [arXiv:2306.08046 \[astro-ph.CO\]](#).
- [107] J. A. Lozano Torres, Generalized emergent dark energy in the late-time Universe, *Mon. Not. Roy. Astron. Soc.* **533**, 1865 (2024).
- [108] J. K. Singh, P. Singh, E. N. Saridakis, S. Myrzakul, and H. Balhara, New Parametrization of the Dark-Energy Equation of State with a Single Parameter, *Universe* **10**, 246 (2024), [arXiv:2304.03783 \[gr-qc\]](#).
- [109] M. Rezaei, Oscillating Dark Energy in Light of the Latest Observations and Its Impact on the Hubble Tension, *Astrophys. J.* **967**, 2 (2024), [arXiv:2403.18968 \[astro-ph.CO\]](#).
- [110] M. Reyhani, M. Najafi, J. T. Firouzjaee, and E. Di Valentino, Structure formation in various dynamical dark energy scenarios, *Phys. Dark Univ.* **44**, 101477 (2024), [arXiv:2403.15202 \[astro-ph.CO\]](#).
- [111] S. Nesseris, Y. Akrami, and G. D. Starkman, To CPL, or not to CPL? What we have not learned about the dark energy equation of state (2025), [arXiv:2503.22529 \[astro-ph.CO\]](#).
- [112] M. Seikel, C. Clarkson, and M. Smith, Reconstruction of dark energy and expansion dynamics using Gaussian processes, *JCAP* **06**, 036, [arXiv:1204.2832 \[astro-ph.CO\]](#).
- [113] S. Nesseris and J. Garcia-Bellido, A new perspective on Dark Energy modeling via Genetic Algorithms, *JCAP* **11**, 033, [arXiv:1205.0364 \[astro-ph.CO\]](#).
- [114] S. Yahya, M. Seikel, C. Clarkson, R. Maartens, and M. Smith, Null tests of the cosmological constant using supernovae, *Phys. Rev. D* **89**, 023503 (2014), [arXiv:1308.4099 \[astro-ph.CO\]](#).
- [115] G.-B. Zhao *et al.*, Dynamical dark energy in light of the latest observations, *Nature Astron.* **1**, 627 (2017), [arXiv:1701.08165 \[astro-ph.CO\]](#).
- [116] Z. Zhang, G. Gu, X. Wang, Y.-H. Li, C. G. Sabiu, H. Park, H. Miao, X. Luo, F. Fang, and X.-D. Li, Non-parametric dark energy reconstruction using the tomographic Alcock-Paczynski test, *Astrophys. J.* **878**, 137 (2019), [arXiv:1902.09794 \[astro-ph.CO\]](#).
- [117] L. A. Escamilla and J. A. Vazquez, Model selection applied to reconstructions of the Dark Energy, *Eur. Phys. J. C* **83**, 251 (2023), [arXiv:2111.10457 \[astro-ph.CO\]](#).
- [118] L. A. Escamilla, S. Pan, E. Di Valentino, A. Paliathanasis, J. A. Vázquez, and W. Yang, Testing an oscillatory behavior of dark energy, *Phys. Rev. D* **111**, 023531 (2025), [arXiv:2404.00181 \[astro-ph.CO\]](#).
- [119] A. N. Ormondroyd, W. J. Handley, M. P. Hobson, and A. N. Lasenby, Nonparametric reconstructions of dynamical dark energy via flexknots (2025), [arXiv:2503.08658 \[astro-ph.CO\]](#).
- [120] A. N. Ormondroyd, W. J. Handley, M. P. Hobson, and A. N. Lasenby, Comparison of dynamical dark energy with Λ CDM in light of DESI DR2 (2025), [arXiv:2503.17342 \[astro-ph.CO\]](#).
- [121] M. Berti, E. Bellini, C. Bonvin, M. Kunz, M. Viel, and M. Zumalacarregui, Reconstructing the dark energy density in light of DESI BAO observations, 2503.13198 (2025).
- [122] E. V. Linder, Exploring the expansion history of the universe, *Phys. Rev. Lett.* **90**, 091301 (2003), [arXiv:astro-ph/0208512](#).
- [123] M. Chevallier and D. Polarski, Accelerating universes with scaling dark matter, *Int. J. Mod. Phys. D* **10**, 213 (2001), [arXiv:gr-qc/0009008](#).
- [124] M. Abdul Karim *et al.* (DESI), DESI DR2 Results II: Measurements of Baryon Acoustic Oscillations and Cosmological Constraints, 2503.14738 (2025).
- [125] K. Lodha *et al.*, Extended Dark Energy analysis using DESI DR2 BAO measurements, 2503.14743 (2025).
- [126] U. Andrade *et al.*, Validation of the DESI DR2 Measurements of Baryon Acoustic Oscillations from Galaxies and Quasars, 2503.14742 (2025).
- [127] D. Scolnic *et al.*, The Pantheon+ Analysis: The Full Data Set and Light-curve Release, *Astrophys. J.* **938**, 113 (2022), [arXiv:2112.03863 \[astro-ph.CO\]](#).
- [128] D. Brout *et al.*, The Pantheon+ Analysis: Cosmological Constraints, *Astrophys. J.* **938**, 110 (2022), [arXiv:2202.04077 \[astro-ph.CO\]](#).
- [129] M. Vincenzi *et al.* (DES), The Dark Energy Survey Supernova Program: Cosmological Analysis and Systematic Uncertainties, *Astrophys. J.* **975**, 86 (2024), [arXiv:2401.02945 \[astro-ph.CO\]](#).
- [130] T. M. C. Abbott *et al.* (DES), The Dark Energy Survey: Cosmology Results with ~ 1500 New High-redshift Type Ia Supernovae Using the Full 5 yr Data Set, *Astrophys. J. Lett.* **973**, L14 (2024), [arXiv:2401.02929 \[astro-ph.CO\]](#).
- [131] B. O. Sánchez *et al.* (DES), The Dark Energy Survey Supernova Program: Light Curves and 5 Yr Data Release, *Astrophys. J.* **975**, 5 (2024), [arXiv:2406.05046 \[astro-ph.CO\]](#).
- [132] D. Rubin *et al.*, Union Through UNITY: Cosmology with 2,000 SNe Using a Unified Bayesian Framework, 2311.12098 (2023).
- [133] A. G. Adame *et al.* (DESI), DESI 2024 VI: cosmological constraints from the measurements of baryon acoustic oscillations, *JCAP* **02**, 021, [arXiv:2404.03002 \[astro-ph.CO\]](#).
- [134] K. Lodha *et al.* (DESI), DESI 2024: Constraints on physics-focused aspects of dark energy using DESI DR1 BAO data, *Phys. Rev. D* **111**, 023532 (2025), [arXiv:2405.13588 \[astro-ph.CO\]](#).
- [135] R. Calderon *et al.* (DESI), DESI 2024: reconstructing dark energy using crossing statistics with DESI DR1 BAO data, *JCAP* **10**, 048, [arXiv:2405.04216 \[astro-ph.CO\]](#).
- [136] M. Cortès and A. R. Liddle, Interpreting DESI's evidence for evolving dark energy, *JCAP* **12**, 007, [arXiv:2404.08056 \[astro-ph.CO\]](#).
- [137] D. Shlivko and P. J. Steinhardt, Assessing observational constraints on dark energy, *Phys. Lett. B* **855**, 138826 (2024), [arXiv:2405.03933 \[astro-ph.CO\]](#).
- [138] O. Luongo and M. Muccino, Model-independent cosmographic constraints from DESI 2024, *Astron. Astrophys.* **690**, A40 (2024), [arXiv:2404.07070 \[astro-ph.CO\]](#).
- [139] W. Yin, Cosmic clues: DESI, dark energy, and the cosmological constant problem, *JHEP* **05**, 327,

- arXiv:2404.06444 [hep-ph].
- [140] I. D. Gialamas, G. Hütsi, K. Kannike, A. Racioppi, M. Raidal, M. Vasar, and H. Veermäe, Interpreting DESI 2024 BAO: late-time dynamical dark energy or a local effect? (2024), arXiv:2406.07533 [astro-ph.CO].
- [141] B. R. Dinda, A new diagnostic for the null test of dynamical dark energy in light of DESI 2024 and other BAO data, *JCAP* **09**, 062, arXiv:2405.06618 [astro-ph.CO].
- [142] H. Wang and Y.-S. Piao, Dark energy in light of recent DESI BAO and Hubble tension (2024), arXiv:2404.18579 [astro-ph.CO].
- [143] Y. Tada and T. Terada, Quintessential interpretation of the evolving dark energy in light of DESI observations, *Phys. Rev. D* **109**, L121305 (2024), arXiv:2404.05722 [astro-ph.CO].
- [144] Y. Carloni, O. Luongo, and M. Muccino, Does dark energy really revive using DESI 2024 data?, *Phys. Rev. D* **111**, 023512 (2025), arXiv:2404.12068 [astro-ph.CO].
- [145] C.-G. Park, J. de Cruz Pérez, and B. Ratra, Using non-DESI data to confirm and strengthen the DESI 2024 spatially flat w_0w_a CDM cosmological parametrization result, *Phys. Rev. D* **110**, 123533 (2024), arXiv:2405.00502 [astro-ph.CO].
- [146] O. F. Ramadan, J. Sakstein, and D. Rubin, DESI constraints on exponential quintessence, *Phys. Rev. D* **110**, L041303 (2024), arXiv:2405.18747 [astro-ph.CO].
- [147] A. Notari, M. Redi, and A. Tesi, Consistent theories for the DESI dark energy fit, *JCAP* **11**, 025, arXiv:2406.08459 [astro-ph.CO].
- [148] L. Orchard and V. H. Cárdenas, Probing dark energy evolution post-DESI 2024, *Phys. Dark Univ.* **46**, 101678 (2024), arXiv:2407.05579 [astro-ph.CO].
- [149] A. Hernández-Almada, M. L. Mendoza-Martínez, M. A. García-Aspeitia, and V. Motta, Phenomenological emergent dark energy in the light of DESI Data Release 1, *Phys. Dark Univ.* **46**, 101668 (2024), arXiv:2407.09430 [astro-ph.CO].
- [150] S. Pourojaghi, M. Malekjani, and Z. Davari, Cosmological constraints on dark energy parametrizations after DESI 2024: Persistent deviation from standard Λ CDM cosmology (2024), arXiv:2407.09767 [astro-ph.CO].
- [151] J. a. Rebouças, D. H. F. de Souza, K. Zhong, V. Miranda, and R. Rosenfeld, Investigating late-time dark energy and massive neutrinos in light of DESI Y1 BAO, *JCAP* **02**, 024, arXiv:2408.14628 [astro-ph.CO].
- [152] W. Giarè, Dynamical Dark Energy Beyond Planck? Constraints from multiple CMB probes, DESI BAO and Type-Ia Supernovae (2024), arXiv:2409.17074 [astro-ph.CO].
- [153] C.-G. Park, J. de Cruz Perez, and B. Ratra, Is the w_0w_a CDM cosmological parameterization evidence for dark energy dynamics partially caused by the excess smoothing of Planck CMB anisotropy data? (2024), arXiv:2410.13627 [astro-ph.CO].
- [154] N. Menci, A. A. Sen, and M. Castellano, The Excess of JWST Bright Galaxies: A Possible Origin in the Ground State of Dynamical Dark Energy in the Light of DESI 2024 Data, *Astrophys. J.* **976**, 227 (2024), arXiv:2410.22940 [astro-ph.CO].
- [155] T.-N. Li, Y.-H. Li, G.-H. Du, P.-J. Wu, L. Feng, J.-F. Zhang, and X. Zhang, Revisiting holographic dark energy after DESI 2024 (2024), arXiv:2411.08639 [astro-ph.CO].
- [156] J.-X. Li and S. Wang, A comprehensive numerical study on four categories of holographic dark energy models (2024), arXiv:2412.09064 [astro-ph.CO].
- [157] A. Notari, M. Redi, and A. Tesi, BAO vs. SN evidence for evolving dark energy (2024), arXiv:2411.11685 [astro-ph.CO].
- [158] Q. Gao, Z. Peng, S. Gao, and Y. Gong, On the Evidence of Dynamical Dark Energy, *Universe* **11**, 10 (2025), arXiv:2411.16046 [astro-ph.CO].
- [159] R. Fikri, E. ElKhateeb, E. S. Lashin, and W. El Hanafy, A preference for dynamical phantom dark energy using one-parameter model with Planck, DESI DR1 BAO and SN data (2024), arXiv:2411.19362 [astro-ph.CO].
- [160] J.-Q. Jiang, D. Pedrotti, S. S. da Costa, and S. Vagnozzi, Non-parametric late-time expansion history reconstruction and implications for the Hubble tension in light of DESI (2024), arXiv:2408.02365 [astro-ph.CO].
- [161] J. Zheng, D.-C. Qiang, and Z.-Q. You, Cosmological constraints on dark energy models using DESI BAO 2024 (2024), arXiv:2412.04830 [astro-ph.CO].
- [162] A. Gómez-Valent and J. Solà Peracaula, Composite Dark Energy and the Cosmological Tensions (2024), arXiv:2412.15124 [astro-ph.CO].
- [163] S. Roy Choudhury and T. Okumura, Updated Cosmological Constraints in Extended Parameter Space with Planck PR4, DESI Baryon Acoustic Oscillations, and Supernovae: Dynamical Dark Energy, Neutrino Masses, Lensing Anomaly, and the Hubble Tension, *Astrophys. J. Lett.* **976**, L11 (2024), arXiv:2409.13022 [astro-ph.CO].
- [164] A. Lewis and E. Chamberlain, Understanding acoustic scale observations: the one-sided fight against Λ (2024), arXiv:2412.13894 [astro-ph.CO].
- [165] A. J. Shajib and J. A. Frieman, Evolving dark energy models: Current and forecast constraints (2025), arXiv:2502.06929 [astro-ph.CO].
- [166] W. Giarè, T. Mahassen, E. Di Valentino, and S. Pan, An overview of what current data can (and cannot yet) say about evolving dark energy, 2502.10264 (2025).
- [167] M. Najafi, S. Pan, E. Di Valentino, and J. T. Firouzjaee, Dynamical dark energy confronted with multiple CMB missions, *Phys. Dark Univ.* **45**, 101539 (2024), arXiv:2407.14939 [astro-ph.CO].
- [168] W. Giarè, M. Najafi, S. Pan, E. Di Valentino, and J. T. Firouzjaee, Robust preference for Dynamical Dark Energy in DESI BAO and SN measurements, *JCAP* **10**, 035, arXiv:2407.16689 [astro-ph.CO].
- [169] W. J. Wolf, C. García-García, and P. G. Ferreira, Robustness of Dark Energy Phenomenology Across Different Parameterizations (2025), arXiv:2502.04929 [astro-ph.CO].
- [170] L. A. Escamilla, D. Fiorucci, G. Montani, and E. Di Valentino, Exploring the Hubble tension with a late time Modified Gravity scenario, *Phys. Dark Univ.* **46**, 101652 (2024), arXiv:2408.04354 [astro-ph.CO].
- [171] E. J. Copeland, M. Sami, and S. Tsujikawa, Dynamics of dark energy, *Int. J. Mod. Phys. D* **15**, 1753 (2006), arXiv:hep-th/0603057.
- [172] A. Lewis, A. Challinor, and A. Lasenby, Efficient computation of CMB anisotropies in closed FRW models, *Astrophys. J.* **538**, 473 (2000), arXiv:astro-ph/9911177.
- [173] W. Hu and I. Sawicki, A Parameterized Post-Friedmann Framework for Modified Gravity, *Phys. Rev. D* **76**,

- 104043 (2007), [arXiv:0708.1190 \[astro-ph\]](#).
- [174] W. Fang, W. Hu, and A. Lewis, Crossing the Phantom Divide with Parameterized Post-Friedmann Dark Energy, *Phys. Rev. D* **78**, 087303 (2008), [arXiv:0808.3125 \[astro-ph\]](#).
- [175] J. Torrado and A. Lewis, Cobaya: Code for Bayesian Analysis of hierarchical physical models, *JCAP* **05**, 057, [arXiv:2005.05290 \[astro-ph.IM\]](#).
- [176] A. Gelman and D. B. Rubin, Inference from Iterative Simulation Using Multiple Sequences, *Statist. Sci.* **7**, 457 (1992).
- [177] A. Lewis, GetDist: a Python package for analysing Monte Carlo samples (2019), [arXiv:1910.13970 \[astro-ph.IM\]](#).
- [178] N. Aghanim *et al.* (Planck), Planck 2018 results. VIII. Gravitational lensing, *Astron. Astrophys.* **641**, A8 (2020), [arXiv:1807.06210 \[astro-ph.CO\]](#).
- [179] N. Aghanim *et al.* (Planck), Planck 2018 results. I. Overview and the cosmological legacy of Planck, *Astron. Astrophys.* **641**, A1 (2020), [arXiv:1807.06205 \[astro-ph.CO\]](#).
- [180] N. Aghanim *et al.* (Planck), Planck 2018 results. V. CMB power spectra and likelihoods, *Astron. Astrophys.* **641**, A5 (2020), [arXiv:1907.12875 \[astro-ph.CO\]](#).
- [181] M. S. Madhavacheril *et al.* (ACT), The Atacama Cosmology Telescope: DR6 Gravitational Lensing Map and Cosmological Parameters, *Astrophys. J.* **962**, 113 (2024), [arXiv:2304.05203 \[astro-ph.CO\]](#).
- [182] F. J. Qu *et al.* (ACT), The Atacama Cosmology Telescope: A Measurement of the DR6 CMB Lensing Power Spectrum and Its Implications for Structure Growth, *Astrophys. J.* **962**, 112 (2024), [arXiv:2304.05202 \[astro-ph.CO\]](#).
- [183] A. Heavens, Y. Fantaye, A. Mootoovaloo, H. Eggers, Z. Hosenie, S. Kroon, and E. Sellentin, Marginal Likelihoods from Monte Carlo Markov Chains (2017), [arXiv:1704.03472 \[stat.CO\]](#).
- [184] W. Giare, *wgcosmo: A set of tools, codes, and methodologies for cosmology* (2025), accessed: 2025-03-30.
- [185] R. E. Kass and A. E. Raftery, Bayes Factors, *J. Am. Statist. Assoc.* **90**, 773 (1995).
- [186] P. Bansal and D. Huterer, Expansion-history preferences of DESI and external data (2025), [arXiv:2502.07185 \[astro-ph.CO\]](#).
- [187] P. Mukherjee and A. A. Sen, A New $\sim 5\sigma$ Tension at Characteristic Redshift from DESI-DR1 BAO and DES-SN5YR Observations (2025), [arXiv:2503.02880 \[astro-ph.CO\]](#).